Biotic and Abiotic Processes In the Formation and Diagenesis of Permian Dolomitic Stromatolites (Zechstein Group, NE England)

Article *in* Journal of Sedimentary Research · September 2013

DOI: 10.2110/jsr.2013.65

CITATIONS
21

READS
1,280

3 authors, including:

Edoardo Perri
Università della Calabria
56 PUBLICATIONS **979** CITATIONS

SEE PROFILE

Maurice Tucker
University of Bristol
234 PUBLICATIONS **13,518** CITATIONS

SEE PROFILE

Journal of Sedimentary Research

Journal of Sedimentary Research, 2013, v. 83, 896-914
Research Article
DOI: http://dx.doi.org/10.2110/jsr.2013.65

BIOTIC AND ABIOTIC PROCESSES IN THE FORMATION AND DIAGENESIS OF PERMIAN DOLOMITIC STROMATOLITES (ZECHSTEIN GROUP, NE ENGLAND)

EDOARDO PERRI,[1] MAURICE E. TUCKER,[2,3] AND MIKE MAWSON[3]
[1]*Dipartimento di Biologia, Ecologia, e Scienze Della Terra, Universita della Calabria, Ponte Bucci 15b, 87036 Rende (CS), Italy*
[2]*School of Earth Sciences, University of Bristol, Bristol BS8 1RJ, U.K.*
[3]*Department of Earth Sciences, Durham University, Durham, DH1 3LE, U.K.*
e-mail: eperri@unical.it

ABSTRACT: **The Crinkly Bed of the Upper Permian Zechstein Group succession (Roker Formation = Hauptdolomit, Z2C) in northeast England is a distinctive 1.4-meter-thick unit that has been interpreted as a stromatolite of microbial origin, or, alternatively, as the result of purely abiotic precipitation. Close examination of this stratigraphically significant unit shows that it is the result of both physical *and* microbial processes, and was deposited in hypersaline shallow water immediately following lowstand evaporite deposition within the Zechstein basin. The internal structure of the Crinkly Bed consists of fine, millimeter scale laminae of alternating clotted peloidal or aphanitic micritic layers and granular laminae composed of silt-size peloids, with rare hollow spheroids. The lamination is extremely regular in thickness and laterally persistent for up to 4 meters. A microbial community composed of coccoid and filamentous microorganisms, inferred from fossil evidence, colonized the original sediment surface. It is suggested that this biofilm was responsible for the precipitation of both the micrite laminae and most of the peloids of the granular laminae; the peloids are consequently interpreted as autochthonous. This interpretation of a microbial origin is consistent with the microstructure and geochemical signatures of the micritic dolomite, which constitutes both the continuous micritic laminae and the peloids themselves. Primary dolomite precipitation is hypothesized to have taken place from marine to slightly hypersaline waters, mediated by bacterial metabolism, similar to the process that operates in modern intertidal microbial mats. The Crinkly Bed shows macro-structures that vary along a continuum from symmetrical to asymmetrical, centimeter scale, ripple-like structures, some showing interference patterns, through to domical and conical structures, more typical of stromatolites. The more ripple-like structures have a lamination of microbial origin identical to that within the domal–conical stromatolites; there is no internal cross lamination. Their origin is equivocal: they could be the result of physical (current- or wave-induced) deformation of a surficial biofilm, or their form could be inherited from true mechanically deposited ripples (not observed) that provided a template for biofilm growth. Changes in the nature and strength of the wave and/or current regime, and possibly in the community structure of the microbial mat, produced this array of microbially induced macrostructures (MISS). The latter, plus the absence of desiccation features indicative of intertidal to supratidal deposition, suggest subtidal sedimentation at a depth of several meters. Intergranular gypsum cement precipitated during early diagenesis, and ferroan sparry dolomite precipitated during burial. Tertiary uplift and the consequent exposure to meteoric waters resulted in the precipitation of calcite cements that replaced gypsum and pre-existing dolomite, probably via the biological mediation of heterotrophic bacteria. The interpretation of this distinctive stratigraphic unit illustrates the difficulty in distinguishing between biotic and abiotic processes in the sedimentary record.**

INTRODUCTION

Both biotic and abiotic processes operate in the genesis and diagenesis of stromatolitic carbonate through the precipitation of minerals, by direct nucleation, or growth mediated in the case of biological processes. The various processes operate syngenetically and epigenetically, and through the trapping and binding of grains by organic substrates, with or without the effects of wave and current activity (Riding 2011). Epibenthic living microbial communities (biofilms or mats) can play a fundamental role in the accretion and early lithification of sediment, as they can mediate the precipitation of micrite as homogeneous laminae, intergranular cement, or autochthonous micritic grains (peloids) (Riding 2000; Dupraz et al. 2009). Biomediated calcite and aragonite in microbial carbonate are well known from the geological record, including modern analogs. Primary microbial dolomite, on the other hand, which is well documented from modern systems, has been poorly recognized in ancient sedimentary successions (McKenzie and Vasconcelos 2009).

During the later stages of diagenesis, when abiotic precipitation of cement is the typically dominant process, some microorganisms do persist in the sediment if there is an availability of nutrients or limiting chemicals for metabolism; epigenetic biomediated minerals may be precipitated in this way (Machel 2001; Konhauser 2007). Sulfate-reducing bacteria (SRB), for example, can eventually oxidize organic matter such as crude oil or methane. Sulfate reduction causes an increase in alkalinity and consequent precipitation of biogenic carbonate, including dolomite, as the microbes eliminate SO_4^{2-} in the pore fluid, removing one of the

Published Online: Month Year
 1527-1404/13/xxx-xxx/$03.00

factors inhibiting dolomite formation (Castanier et al. 2000; Ziegenbalg et al. 2010).

Macroscopic lamination and growth forms are the best-known features of ancient and modern stromatolites, which are undoubtedly comparable in terms of morphology (Allwood et al. 2006; Awramik 2006). Petrographic microfabrics of micrite vary from clotted peloidal to laminated, to aphanitic, and such features may be indicative of a biotic origin. However, several ultrastructural studies of microbial stromatolites have demonstrated that these micritic fabrics can be a mixture of biotic and abiotic mineral precipitates (Spadafora et al. 2010; Perri et al. 2012a, 2012b). In some cases, microspar and even sparry calcite are produced through biologically mediated reactions (Brasier et al. 2011; Manzo et al. 2012).

Ancient microbialites normally lack unambiguous evidence for the original microbes in the form of fossils, an exception being some early Paleozoic microbialites. They also rarely retain their primary geochemical signatures. For all these reasons, testing the biogenicity of ancient microbialites can be very difficult and contentious.

This paper focuses on a distinctive Upper Permian (Zechstein) stromatolitic deposit of the Roker Formation that is exposed in Northeast England. This 1.4-meter-thick unit, called the "Crinkly Bed" (Smith 1995), exhibits a range of centimeter-scale macrostructures, from obviously stromatolitic domes and cones, through to various ripple-like features. However, these macro-structures, as well as the laminae, have been interpreted as being largely the result of abiotic processes, formed through "chemogenic precipitation in the absence of microbial mats" (Pope et al. 2000, p. 1139) and even as travertine (Harwood et al. 1990). Although the Zechstein carbonate–evaporite deposits have usually undergone a complex diagenetic history (Tucker and Hollingworth 1986; Lee and Harwood 1989), the Crinkly Bed shows excellent preservation of grains and microbial fossils, and is thought likely to retain its original geochemical signatures.

Study of this stromatolitic unit shows that microbialites commonly are more complicated than they first appear. Analyses of the fabrics and structures are relevant to other microbialite formations in the stratigraphic record.

As discussed by Pope et al. (2000), Sarg (2001), and Warren (2006), thick microbial–stromatolitic carbonate units are a characteristic feature of carbonate evaporite successions throughout the stratigraphic record. They are an important type of hydrocarbon reservoir too, because they commonly are extremely porous, and can even form source rocks (Słowakiewicz and Mikołajewski 2011). Examples in other parts of the geological record include: the upper Precambrian Ara Formation of Oman, the Silurian Niagaran reefs of the Michigan Basin, and the Devonian Muskeg Nisku reefs in Western Canada, as well as the recent discoveries of microbial carbonate reservoirs in the Cretaceous of the Santos Basin, offshore Brazil, and their equivalents in offshore Angola (Wasson et al. 2012). Thus, an understanding of the occurrence of microbialites, their features, extent, and geometry, is also of interest for petroleum exploration.

GEOLOGICAL AND STRATIGRAPHIC SETTING

The Upper Permian Zechstein Group of Northeast England comprises a succession of carbonate and evaporite cycles deposited along the western margin of the Zechstein Sea under a hot and arid climate (Smith 1981; Tucker 1991) (Fig. 1A). The first-cycle carbonate (Z1C) in the Durham province consists of two formations, the Raisby and Ford formations (= Zechsteinkalk of the southern North Sea and continental Europe), with the former representing distally steepened carbonate ramp facies and the latter a reef-rimmed shelf deposit (Tucker and Hollingworth 1986). Fore-reef debris of blocks and skeletal sand generated clinoforms during highstand deposition, and these prograded several hundred meters into the basin. On the basin floor itself, the only equivalent deposits are a thin pisolitic–oncolitic, stromatolitic mudstone, 10–30 cm thick (maximum 60 cm), known as the Trow Point Bed (Smith 1986). Behind the reef, oolitic sand and lime mud were deposited in the shelf lagoon, which was some 10–15 km across (Smith 1980).

After development of the first-cycle carbonate in the Durham Province, the first-cycle evaporites (Hartlepool Anhydrite, Z1A, = Werra Anhydrit) were deposited, terminating the first Zechstein cycle. The evaporites reach 100 m in thickness and were deposited as a lowstand wedge, some 20–30 km across, against the shelf-margin slope of the Ford Formation reef (Tucker 1991). Much of the anhydrite is nodular, but the anhydrite could represent a replacement of selenitic gypsum, precipitated in shallow water. Laminated microbial dolomite occurs in the Hartlepool Anhydrite, and is commonly folded and contorted, indicating downslope mass movement.

In southeast Durham, a prominent Boulder Conglomerate (Smith 1995) with a disconformity at its top forms the uppermost part of the Ford Formation. This is succeeded by shallow subtidal to intertidal facies, mostly consisting of a variety of microbially laminated carbonate, generally ~ 1 m thick. These rocks have many vugs, indicating that they formerly contained much sulfate, suggesting deposition in a high-salinity environment. The distinctive 1.4-meter-thick Crinkly Bed itself overlies this succession (Fig. 1B, C) and in turn is overlain by over 15 m of interbedded stromatolitic carbonate and packstone–grainstone. Succeeding rocks formed in a variety of shallow-water environments; ooid shoal facies cap the succession, which is up to ~ 60 m thick in total. The Crinkly Bed is exposed at five localities, on and close to the coast of County Durham in northeastern England: Hawthorn Quarry (NZ 437463), Blackhall Rocks (NZ 470390), Hesleden Dene (NZ 460440), Crimdon Dene (NZ 470370), and Hart Quarry (NZ 477345), spread over a northwest–southeast distance of some 13 km. The Crinkly Bed appears to have formed within a narrow facies belt, up to 1.5 km wide, parallel to, and just behind, the former Ford Formation (Z1) shelf margin. This was likely a lagoonal-type environment passing landwards (west) to wide tidal flats and sabkhas (Smith 1981).

The matrix to the Boulder Conglomerate contains reefal fossils of Z1 age, confirming that it is part of the first-cycle carbonate (Z1C). All the strata above the discontinuity at the top of the Boulder Conglomerate, including the microbialites with the Crinkly Bed, are assigned to the second Zechstein cycle carbonates (Z2C) and constitute the Roker Formation (Mawson and Tucker 2009; = Hauptdolomit); this succession occurs in the landward part of the Roker platform and forms a succession up to ~ 60 m thick. To the east, more basinward equivalents of the Crinkly Bed consist of laminated microbialite originally interbedded with anhydrite, which is now present only in the subsurface because it has undergone dissolution at outcrop. These rocks are affected by collapse brecciation as a result of dissolution of the once-present underlying Z1C Hartlepool Anhydrite, which took place mostly in the Tertiary. This stratigraphic arrangement confirms a Z2C age for the Crinkly Bed.

In many places, the basal Z2C Roker strata, including the basal Crinkly Bed, rest disconformably on the Boulder Conglomerate, but in part of Hawthorn Quarry and Hart Quarry the Boulder Conglomerate is absent and they rest directly on reefal facies. In Hesleden Dene, paleogeographically the most landward of the exposures, the Z2C with the Crinkly Bed near its base overlies supratidal fenestral facies deformed into mega-tepee structures (Mawson and Tucker 2009). Lenses of pisoids (up to 2 cm in diameter) occur locally within and upon the upper surface of the Crinkly Bed.

The Boulder Conglomerate reaches ~ 7 m in thickness and is composed of clasts of Z1 reef-flat and reef facies. It has a predominantly clast-supported fabric, but the top ~ 1 meter is generally matrix-supported and may contain some terrigenous clay and quartz silt. The

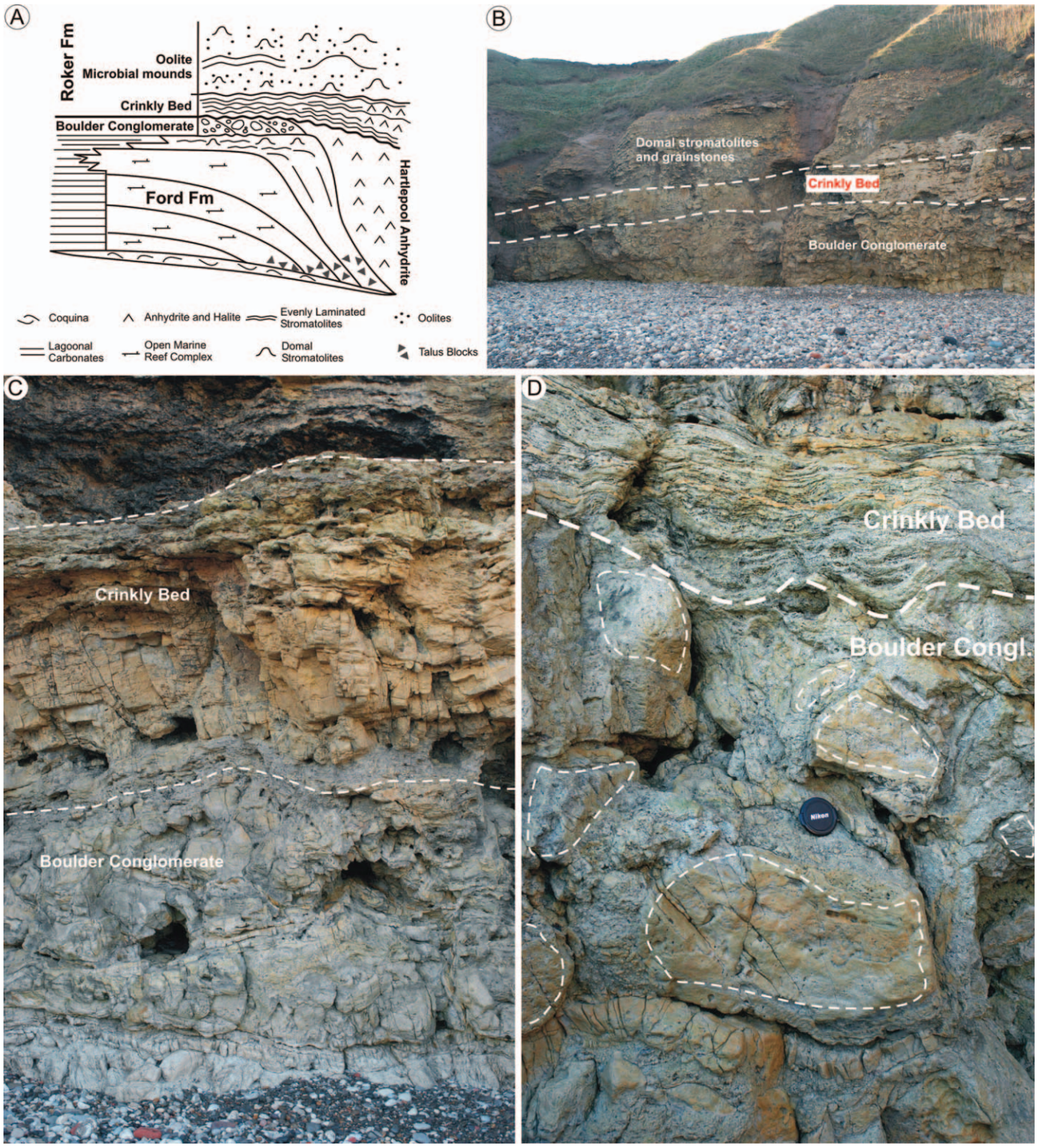

FIG. 1.—Context and field views of the Crinkly Bed from the coast just south of the Gin Cave, Blackhall Rocks, Co. Durham. **A)** The stratigraphic position of the Crinkly Bed in the Zechstein domain of NE England. **B)** Panoramic view of an outcrop of the lower part of the Roker Formation (Z2C), composed of the 1.4-meter-thick Crinkly Bed and succeeding domical stromatolites and grainstones. All of these overlie the Boulder Conglomerate, the topmost bed of the Ford Formation (Z1C). Height of cliff is 50 m. **C)** Close-up field view of the Boulder Conglomerate (Z1C) showing 2 m of boulders and microbial sheets, succeeded by a nonplanar disconformity, first dashed line (= sequence boundary between Z1C and Z2C). This surface is overlain by coarse microbial laminites (0.5 m) and then the Crinkly Bed (1.5 m thick), of the Z2C. Height of cliff 5 m. **D)** Typical aspect of the Boulder Conglomerate (clasts outlined with dashed lines) composed of clasts of Z1 reef facies coated by laminated microbialite, overlain by microbialites and the Crinkly Bed. Height of exposure 1.5 m.

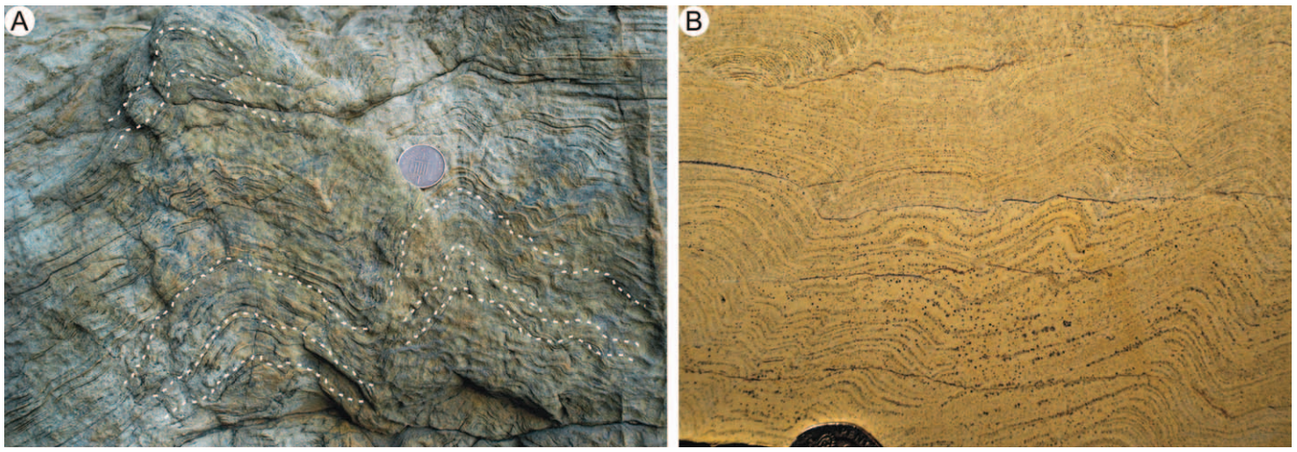

FIG. 2.—Crinkly Bed lamination. **A)** Field view of domal to columnar stromatolitic structures with crinkled and irregular lamination. Coin is 20 mm in diameter. **B)** Polished surface, perpendicular to bedding, with persistent lamination showing undulations of varying shape, which on the bedding surface are seen as ripple-like structures. Height of view 10 cm.

clasts are mostly of cobble to boulder size, and, depending on the locality, are rounded to subangular (Fig. 1D). Many clasts have a coating of laminated microbialitic carbonate (from a few millimeters up to 5 cm thick). The Boulder Conglomerate is thought to have formed in a high-energy surf-zone environment and to be analogous to boulder–coral-rampart deposits associated with modern coral reefs.

In the succession above the Crinkly Bed, there are flat-topped domical stromatolites, up to 18 m in width (commonly $>$ 5 m) with $<$ 1 m of relief. The constituent laminae of these domes are mostly poorly preserved. Grainstone, consisting predominantly of pisoids, and often containing wave ripples, is associated with the stromatolitic buildups and forms units up $\sim$ 3 m or more thick. One feature of the grainstone is that it shows a fitted texture, with the grains strongly flattened. This texture (vadose compaction) is probably related to synsedimentary subaerial exposure to meteoric diagenesis, as has been recorded from the Zechstein of the Netherlands by Clark (1980).

METHODS

Thin sections of the stromatolites were used for microfacies characterization using traditional petrographic methods. Scanning electron microscope (SEM) studies of the nanofabrics on polished thin sections and freshly broken surfaces used an FEI-Philips ESEM-FEG Quanta 200F, operating in a range of 5–20 kV with working distance between 6 and 15 mm. SEM samples were carbon- or gold-coated, respectively, depending on whether they were prepared for microanalysis or for textural study. Mineral composition of bulk samples was determined using X-ray diffraction (Philips PW1730 diffractometer). The major-element and trace-element contents were determined by X-ray fluorescence (Philips PW1480). Semi quantitative element analyses of micron-sized spots used an EDAX energy-dispersive X-ray spectrometer (EDS) operating at 20 kV with a working distance of 12 mm, during SEM observations. Carbon and oxygen isotope analyses were carried out on selected samples: 8–10 mg of sample dissolved at 25°C in 100% orthophosphoric acid for 12 h (calcite samples) or 72 h (dolomite samples). For mixed-mineralogy samples, CO_2 was extracted after 2 h for the calcite fraction and after 72 h for the dolomite fraction. CL studies used a Technosyn instrument.

MICROSTRUCTURE OF CRINKLY BED LAMINAE

Lamination below the Crinkly Bed is less well developed, irregular in thickness, and discontinuous, whereas upwards, from the base of the Crinkly Bed, the lamination quickly becomes more regular, continuous, and distinctly isopachous (Figs. 2A, B, 3A, B). The Crinkly Bed laminae contain numerous cavities with irregular to subpolygonal shapes (Fig. 3A–C). Their dimensions vary from a few microns up to several millimeters; some are empty and others contain cement. Larger cavities (up to 10 cm) also occur within the bed, oval to irregular in shape.

At the finest scale, the lamination of the Crinkly Bed essentially consists of an alternation of micritic and granular laminae (Figs. 3C, D, 4). Grains are chiefly peloids composed of micritic to microsparitic dolomite crystal aggregates, most of which are spheroidal although some are lens-shaped (probably pseudomorphs after sulfate crystals) (Figs. 3C, E, 4). Empty spheroidal structures are locally present (Fig. 4B). Grains are generally of silt size (20–100 μm); only the empty spheres are larger, reaching 100–300 μm in diameter, with walls 10–20 μm thick. Detrital silt size quartz grains occur rarely.

In the first decimeter of the Crinkly Bed itself, multi-millimetric micritic laminae, generally thicker here than higher up, alternate with the granular laminae. The micrite laminae show a micro-peloidal texture and contain abundant cavities, up to several millimeters in size. These laminae alternate with thinner and darker laminae of very fine-grained crystals, which generate a crude lamination (Fig. 3A). The micro-clotted to peloidal texture is composed of dolomicritic peloids tens of microns in diameter, which are isolated or in clumps with irregular intergranular porosity. The grains show the classic antigravitational pattern of microbial peloids, appearing suspended and hanging from cavity roofs (Fig. 5A) (Riding and Tomas 2006). This feature is typical of autochthonous microbial peloids, as commonly observed in microbialites.

Intergranular pores are normally empty in the granular laminae, except where gypsum cement with yellow-brown, acicular, sub-euhedral crystals or microcrystals is preserved (Figs. 5B, C, 6E, F). Relicts of gypsum crystals occur within cavities, suggesting that the latter were previously completely filled by gypsum.

In the upper part of the bed, homogeneous and continuous micritic laminae, 0.1–0.5 mm thick, alternate regularly with thicker granular laminae (0.3–0.9 mm), giving the characteristic laminated aspect to the deposit (Fig. 3B). The laminae are generally parallel and extremely continuous (for at least 4 meters). Locally, there are some subtle stratigraphic changes in the relative thickness between micritic and granular laminae. The lamination is planar to undulating to corrugated, and follows the mesoscale (centimeters) structures of the ripple-like

features through to domes and cones, described later. Cross lamination is absent, and crosscutting or truncation of laminae is rare. There is also an absence of polygonal (desiccation) cracks and sheet cracks (laminar fenestrae). Rare intraclasts reach up to 3 cm in length, and occur in depressions within the macrostructures.

Late diagenetic sparry calcite crystals occupy some of the pores in the granular layers and develop upwards into larger and more continuous mosaics. In cases, these crystals totally replace the granular layers and fill the voids after gypsum (Fig. 7).

PETROGRAPHY AND COMPOSITION OF THE CRINKLY BED

The Crinkly Bed is composed mainly of dolomite and calcite (up to 97% of the rock volume), with the remainder being clay minerals, oxides, quartz, and rarely gypsum (Table 1). The chemical composition of bulk samples is presented in Table 1.

Dolomite

The dolomite is generally micritic, irrespective of lamination type (granular or micritic laminae), and consists of very small, fabric-preserving, light-gray-yellow, anhedral to subhedral crystals, from less than one micron to several tens of microns in size (Fig. 6A, B). Larger, clear, subhedral sparry dolomite crystals, up to a millimeter across, are locally present, and tend to fill primary pore space (Fig. 6C). EDS microanalyses show a general homogeneous Mg/Ca ratio in the micritic dolomite, with an average Ca content of 54 mole%, although several values are $>$ 60 mole%. Fe, Na, and Sr are generally absent or below the detection limit, although $\sim$ 0.5 mole% of Na has been recorded. On the other hand, the coarse sparry dolomite crystals have a lower Ca content, with a measurable Mg excess reaching 55 mole%, and a low Fe content (0.5–1 mole%). Within the dolomite crystals are common euhedral to subhedral, micron- to submicron-size inclusions of fluorite and halite. In addition, there are locally anhedral inclusions of Mg calcite (Mg $\sim$ 10 mole%) (Fig. 6D).

Relicts of subhedral gypsum crystals (Fig. 5C, D), observed in thin section, and confirmed with SEM, have micron-size elongate swallow-tail shapes, whereas microcrystalline gypsum is composed of 1–2 micron, needle-shaped crystals, in aggregates, with locally disoriented crystals (Fig. 6E, F). The average molar atomic composition is 54% Ca and 46% S. Grains and micrite crystals surrounded by gypsum are composed of Ca-rich dolomite.

Calcite

In thin sections of the Crinkly Bed, calcite cements are drusy, equant, clear crystals that initially filled primary pore spaces, mainly along the granular laminae and in rectilinear-shaped cavities (Fig. 7A). In some places, there has been wholesale replacement of the Crinkly Bed by sparry calcite, although commonly the micritic laminae have been left almost intact (Fig. 7C). Calcite is generally inclusion-free and non-ferroan but shows a constant low-Mg content in a range of 1–6 mole%, particularly along the transition zones with the dolomite.

The microstructure of the calcite crystals is generally homogeneous, although cleavage planes are conspicuous. However, along interfaces with dolomite and gypsum crystals the calcite shows a distinct microstructure of elongate and polygonal micro-cavities in transverse section. In addition, the calcite has a granular texture, consisting of coalescing spheroidal to irregular nanocrystals, 0.1–0.4 microns across (Fig. 8).

Abundant micro-scale crystal aggregates of (Fe, Mn) oxideshydroxides and (Fe, Mg, Al) silicate minerals are widespread and are more or less opaque in thin section (Figs. 2E, 3C, E, 5A). These precipitates range from poorly ordered to crystalline phases that vary from acicular (Fe-rich) to platy in shape (Al-Si rich) (Fig. 9).

Cathodoluminescence

CL images reveal that the micritic dolomite is uniformly very dull or nonluminescent, whereas the coarser sparitic dolomite crystals show a blotchy luminescence (Fig. 7). The equant crystals of calcite show several growth zones of different luminescence, with an early wide, bright orange zone containing dull subzones 10–20 microns thick. A concentric pattern is common around dark clasts or centers of cementation. The bright orange zone is followed by much thinner (5 micron) white to orange zones that are interlayered across polygonal boundaries with dull orange subzones. A dull zone characterizes the outer part of the crystals, which in cases extends for several 100 microns (Fig. 7B).

Isotope Measurements

Isotopic data were collected from nine bulk samples (Table 2 and Fig. 10). Samples H1 to H7, in stratigraphic order from Blackhall Rocks, represent microbial laminites from within the Boulder Conglomerate (H1 and H2), up through the Crinkly Bed to its top (H7). Sample CA was obtained by microsampling submillimeter, dogtooth isopachous calcite crystals from a cavity in the H5 hand sample. Sample LP, a stromatolitic facies very similar to the H-samples, comes from the Crinkly Bed in Hawthorn Quarry.

Pure or almost pure dolomite samples (H1 and H5) show average values in PDB: $\delta^{18}O = +1.1‰$ ($\pm$ 0.3) and $\delta^{13}C = +6.9‰$ ($\pm$ 0.3). The calcite (CA) has $\delta^{18}O = -6.2‰$ and $\delta^{13}C = -7.4‰$, whereas the sparry calcite present in the laminae and cavities from near the top of the Crinkly Bed in sample H7 has $\delta^{18}O = -4.9‰$ and $\delta^{13}C = -4.0‰$.

BIOTIC MICROSTRUCTURES

The micritic laminae of the Crinkly Bed contain remains of problematic coccoid and filamentous microfossils (Fig. 11). The latter consist mainly of nonseptate, empty, subspherical tubes of variable length, located along the micritic laminae (Fig. 11A). Solid micritic filaments are preserved transverse to the granular laminae, where they may show a fan-like subvertical arrangement (Fig. 11B). Their diameters generally range between 8 and 20 μm. The filaments following the laminae could be attributed to the genus *Girvanella*, whereas the fan-like arrangement is reminiscent of the genus *Ortonella,* although that is more tubiform (Wray 1977). Nonmineralized filamentous organic matter relicts of uncertain origin are also present (Fig. 11C). Some filaments $\sim$ 1 μm in diameter, and molds of bacteria like fossils, appear to consist of phosphate (probably apatite) (Fig. 11D). Subspherical empty molds 3–5 μm in diameter (Fig. 11E), could be coccoid bacterial forms, in view of their small dimension. There are rare, larger empty tubes, 150–200 μm in diameter, that cut across several laminae, and these could have been formed by a boring or burrowing organism (Fig. 11F).

CRINKLY BED MACROSTRUCTURES

At the centimeter to decimeter scale the Crinkly Bed shows a variety of distinctive structures (Fig. 12), which vary from ripple-like features formed through physical processes, through to domical and conical structures that are more typical of stromatolites. On a larger, meter scale, very gentle mounded features are present locally (notably the Blackhall Rocks locality).

The ripple-like forms have two scales. Larger-scale structures vary from linear, ridge-like features up to a meter long (Fig. 12A), to more commonly elliptical-shaped features that are up to several tens of centimeters long (Fig. 12B). There is a broad north–south trend of the straight crests of these larger structures at Blackhall Rocks. Superimposed

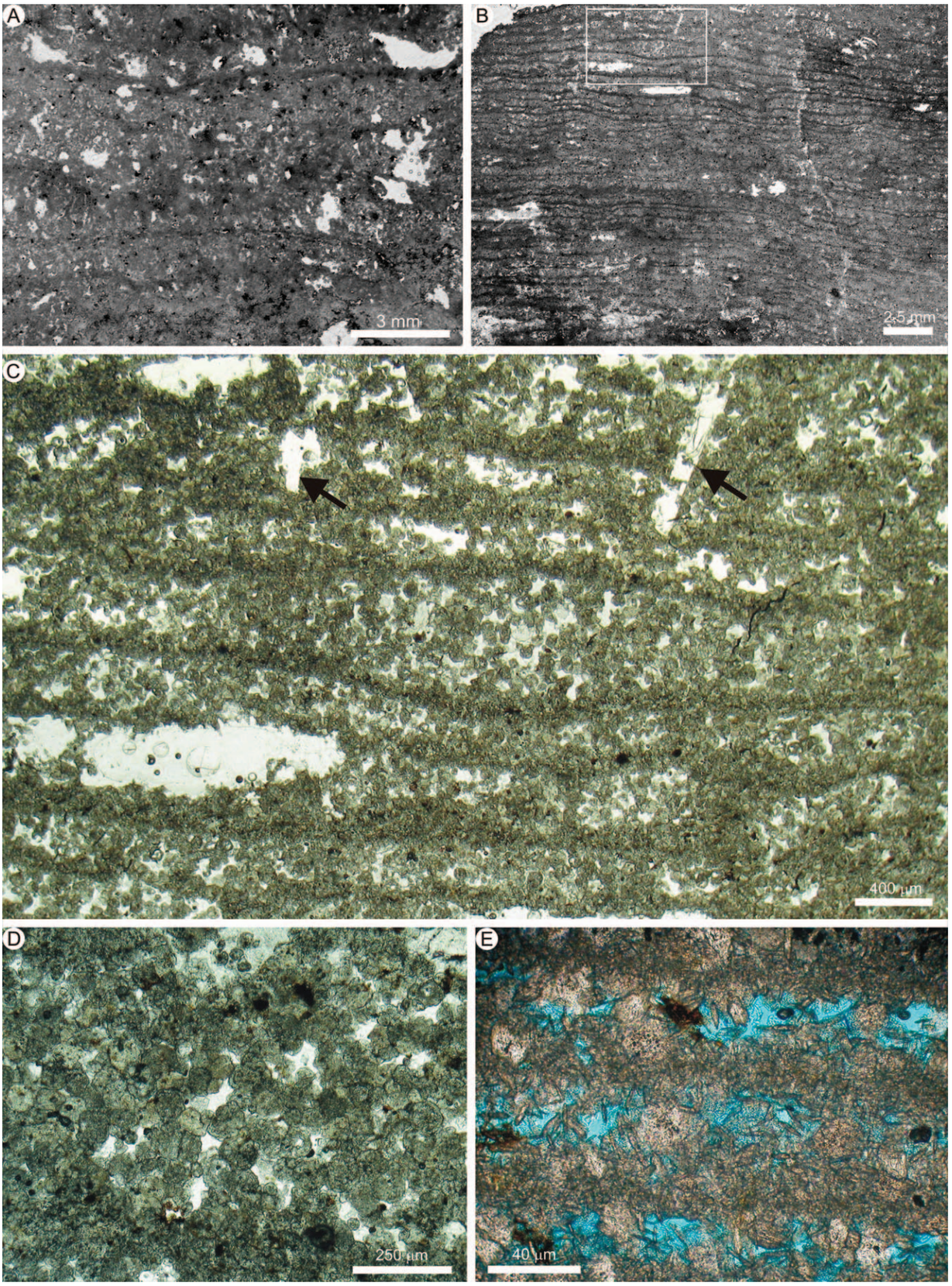
A
3 mm
B
2.5 mm
C
400 µm
D
250 µm
E
40 µm

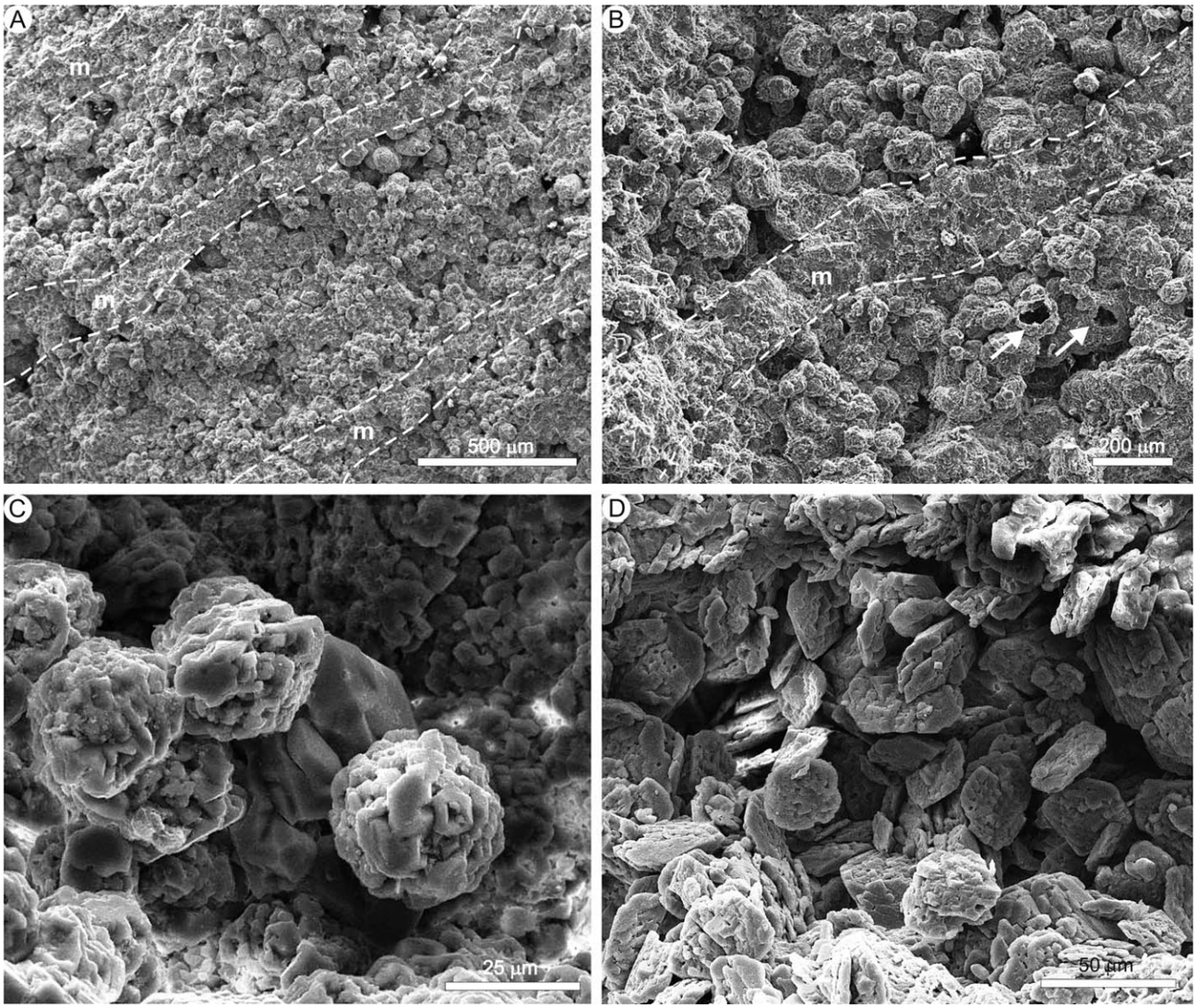

FIG. 4.—SEM images of the microstructure of the lamination on fresh surfaces. **A**, **B)** Alternation of dolomicritic layers (labelled "m") and granular layers. Note in part B the hollow spherical grains (white arrows). **C)** Close-up view of rounded micritic–microsparitic grains. **D)** Lens-shaped grains (probably pseudomorphs after sulfates).

on these are smaller-scale, commonly symmetric, ripple-like features with a wavelength of 1.5–5 cm and straight to curved to bifurcating crest patterns (Fig. 12A, B). In some cases, there are two orientations of crests, which produce interference patterns, and there are structures developed which are reminiscent of "tadpole nests." The crests of these ripple-like forms are commonly rounded, and the troughs are smooth and concave up. There are also asymmetric features with curved crests (a linguoid shape), 1.5–10 cm across, which have a similar spacing (Fig. 12C). The steeper sides are nearly vertical in some cases, and up to 4 cm high (Fig. 12C). The crests of these various types of small ripple-like macrostructures show some local preferred alignment, but overall (e.g., Fig. 12A, B) they display no persistent preferred orientation; instead, their crest orientation is consistent with the orientation and shape of the larger ripple-like structures (Fig. 12).

The lamination in these ripple-like structures (Fig. 2) is identical to that forming the more obviously stromatolitic structures, described below.

←

FIG. 3.—Microstructure of Crinkly Bed lamination. Thin-section photomicrographs showing **A**) the poorly developed, irregular thickness and discontinuous lamination at the base of the Crinkly Bed (see also Fig. 5 for details), and **B)** the regular, continuous, and distinctly isopachous lamination in the remaining part; white areas are cavities. **C)** Close-up view white rectangle of part B showing the alternation of thin, micritic dark laminae with thicker granular laminae. Note porosity (clear white areas) and the subpolygonal shapes of some cavities (arrow). **D)** Close-up view of grains, most of which are rounded. White areas are porosity. **E)** Alternation of micritic and granular layers, with rounded to lens-shaped grains. Blue areas are porosity. Note in parts C–E widespread opaque minerals consisting of (Fe, Mn) oxides and hydroxides.

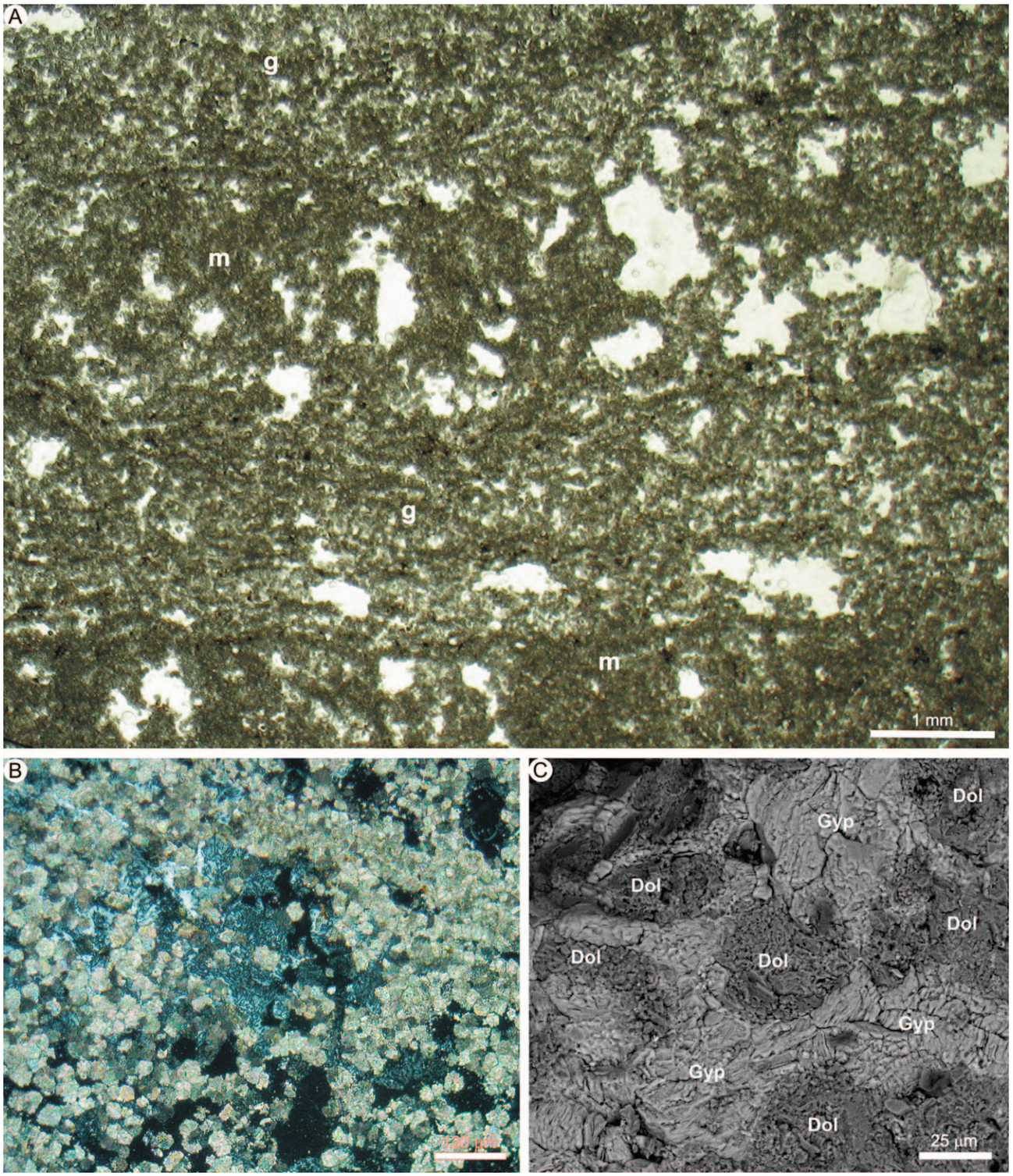

FIG. 5.—Microstructure of Crinkly Bed lamination. **A)** Alternation of micritic (m) and granular layers (g). The micritic layers show a microclotted to peloidal texture with several cavities with subpolygonal shape. White areas are porosity. **B)** Relicts of gypsum (gray-colored mineral) filling cavities and the intergranular space among dolomitic grains (high interference colors). Dark areas are porosity. Thin section, crossed polars. **C)** SEM view (back-scattered electron image) of relicts of gypsum (Gyp) among dolomitic grains (Dol).

Undulations and corrugations in the lamination persist vertically for several tens of centimeters.

Small domical structures, common on bedding surfaces, are up to 10–15 cm across and up to 8–10 cm high; they grade into the linguoid-shaped features noted above (Fig. 12C). The lamination in some of these structures is more crinkled and irregular, giving them a more typical "stromatolitic" appearance, with the characteristic convex-upward growth (Fig. 12C); the majority of the laminae are still isopachous, and there are no breakages or disruptions. These domical structures are locally developed into cones; some have an almost mamillary shape, but with a prominent pimple–nipple on the top, 0.5 cm across and high (Fig. 12C). These sites of local upward growth are locally asymmetric. Polygonal structures arising from expansion (or contraction) of a surficial mat are absent.

INTERPRETATIONS AND DISCUSSION

Origin of the Crinkly Bed Lamination

The Crinkly Bed lamination, which includes alternating thinner micritic and thicker granular layers, overall would have been dominantly granular at the time of deposition. The type of granular–micritic lamination in the Crinkly Bed is rare in the geological record of stromatolites (Awramik and Riding 1988; Riding et al. 1991; Riding 1994; Riding 2000) but seems common in modern stromatolites formed on tidal flats, in tidal channels, and in open-marine settings with normal salinity, as around Lee Stocking Island (Seong-Joo et al. 2000) and other areas in Exuma Sound (Bahamas). Reid et al. (1995) and Visscher et al. (1998) described well-laminated structures from these areas that are composed mainly of episodically lithified fine (125–250 μm) carbonate sand layers (2–3 mm thick) that alternate with lime mud layers (20–60 μm thick). Moreover, the sand grains, mostly of bioclastic origin, are commonly intensely microbored, truncated, and micritized. Three stages in the formation of these intertidal stromatolites were recognized (Reid et al. 2000): 1) a filamentous cyanobacterial (*Schizothrix* sp.) dominated community where the grains are trapped and bound, having a relatively low biomass, low photosynthetic rates, and few associated heterotrophic organisms; 2) a more diverse community, where aerobic and anaerobic microbes are abundant (e.g., sulfate-reducing bacteria), which produce much of the extracellular polymeric substance (EPS) that is lithified early to form a thin crust of lime mud; and 3) a highly developed community, which includes coccoid endolithic cyanobacteria (e.g., *Solentia* sp.), forming a thicker lithified lamina through boring and binding of the grains and precipitation of aragonite.

Within the Crinkly Bed, the filamentous and coccoid remains of cyanobacterial forms are very similar to those that characterize the microbial communities of the Exuma stromatolites. Filamentous forms in the Crinkly Bed occur both in the micritic laminae (subhorizontally) and in the granular laminae (subvertically), indicating a potential role in the trapping and binding of grains, and in the production of micrite (Fig. 9).

The strong similarity of both the sedimentary microfabrics and inferred microbiological components of the Crinkly Bed with modern intertidal–subtidal Bahamian stromatolites suggests that the Crinkly Bed could be regarded as an ancient counterpart of this type of organo-sedimentary deposit. Although quite different from the Exuma tidal-channel, high-relief domal stromatolitic buildups, which reach over 2 m above the seafloor, there are conical to domal growth structures in the Crinkly Bed that resemble the small-scale mats in the nearshore, shallow back-reef area of Highborne Cay (Andres and Reid 2006). Here, microbial mats grow with 5–10 cm of relief, in the form of ridges 10–20 cm wide, coalescing or branching in plan view, and are surrounded by rippled sand. Accommodation space, sediment grain size, and hydrodynamics, together with the surface colonization by macro-algae and boring organisms, have been identified as the physical and biological factors controlling the shape of these modern stromatolites.

In the Crinkly Bed, the granular layers are composed mainly of peloids. Peloids may be fecal pellets or originate from micritization of allochthonous clasts, but, in many modern and ancient "grain-lacking" stromatolites (fine-grained stromatolites of Riding 2000) they are autochthonous, a by-product of microbially mediated mineral precipitation in the microbial mats and biofilms (Dupraz et al. 2004; Riding 2011; Perri and Spadafora 2011). The peloidal fabric usually is composed of fine micritic clots (subspherical or irregular in shape), clearly biotic in origin, that are surrounded by microspar (abiotic) and irregular cavities. The mineralogy of the peloids and microspar is either the same (usually calcite) or different (aragonite, calcite or dolomite), depending on the local chemical conditions. Lamination in this type of autochthonous, grain-free stromatolite varies from coarse and irregular with indistinct laminae, to crenulated (e.g., stromatolites in Lagoa Vermelha in Brazil; Spadafora et al. 2010), to submillimetric, isopachous, and smooth, the latter of which originated from the alternation of thin aphanitic micritic layers and thicker peloidal layers (e.g., stromatolites from Marion Lake, Australia, Perri et al. 2012b).

A similar mechanism of formation could be inferred for the origin of the peloids of the Crinkly Bed (cf. Perri et al. 2012b). In view of the generally very regular spherical form of Crinkly Bed peloids, the mechanism of formation of this particular stromatolitic peloidal fabric can be best interpreted by comparison with biotically mediated, autochthonous micritic and microsparitic grains (peloids) that have been recently documented from microbial mats of the tidal flats of Abu Dhabi (Bontognali et al. 2010). These peloids are composed of aggregates of microcrystals forming well-developed spheroids ranging in size from 10 to 500 microns, which originated randomly within a laminated microbial mat or formed distinct millimetric layers along which they coalesced together. The composition of these modern grains is dolomite, and its precipitation could have taken place (1) within the epibenthic living mat as a consequence of the metabolism of sulfate-reducing bacteria (SRB), which eliminates SO_4^{2-}, an inhibiting factor in dolomite precipitation, and increases alkalinity to allow the precipitation of primary (microbial) dolomite; or (2) within the buried nonliving mat, where SRB are inactive, by the mineralization of the degrading EPS (Bontognali et al. 2010). Since EPS plays a key role in the origin of such grains in this shallow-burial environment, these grains can be considered as biologically mediated too, through a process of microbially induced or influenced mineralization (Dupraz et al. 2009). In addition to autochthonous dolomitic grains, the microbial mats contain carbonate and noncarbonate sand grains of detrital origin, trapped and bound on the mat, as well as layers of discoidal gypsum mush. The rare silt-size allochthonous grains in the Crinkly Bed could have been supplied by wave and current activity (or wind). The composition and fabric of the peloidal laminae in the Abu Dhabi microbial mats are very similar to the granular layers of the Crinkly Bed, suggesting a similar mechanism of formation, including the primary origin of the dolomite grains. Moreover, Abu Dhabi peritidal sediment contains abundant evaporite minerals (halite, gypsum) that reflect the well-known hypersaline environment of the sabkha, and these have also been observed as inclusions and molds after dissolution in the Crinkly Bed. Crinkly Bed dolomite peloids are similar to those that Wright (1999) observed forming in hypersaline Coorong lakes via SRB mediation, and which were also reproduced in laboratory culture (Wright and Wacey 2005). Spheroids of primary microbial dolomite, comparable to the Crinkly Bed spheroids, have also been obtained in microbial cultures of moderately halophytic aerobic bacteria (Sánchez-Román et al. 2008). Finally, similar spheroids of primary (inferred) dolomite have been documented in Messinian stromatolites of hypersaline environments (Olivieri et al. 2010).

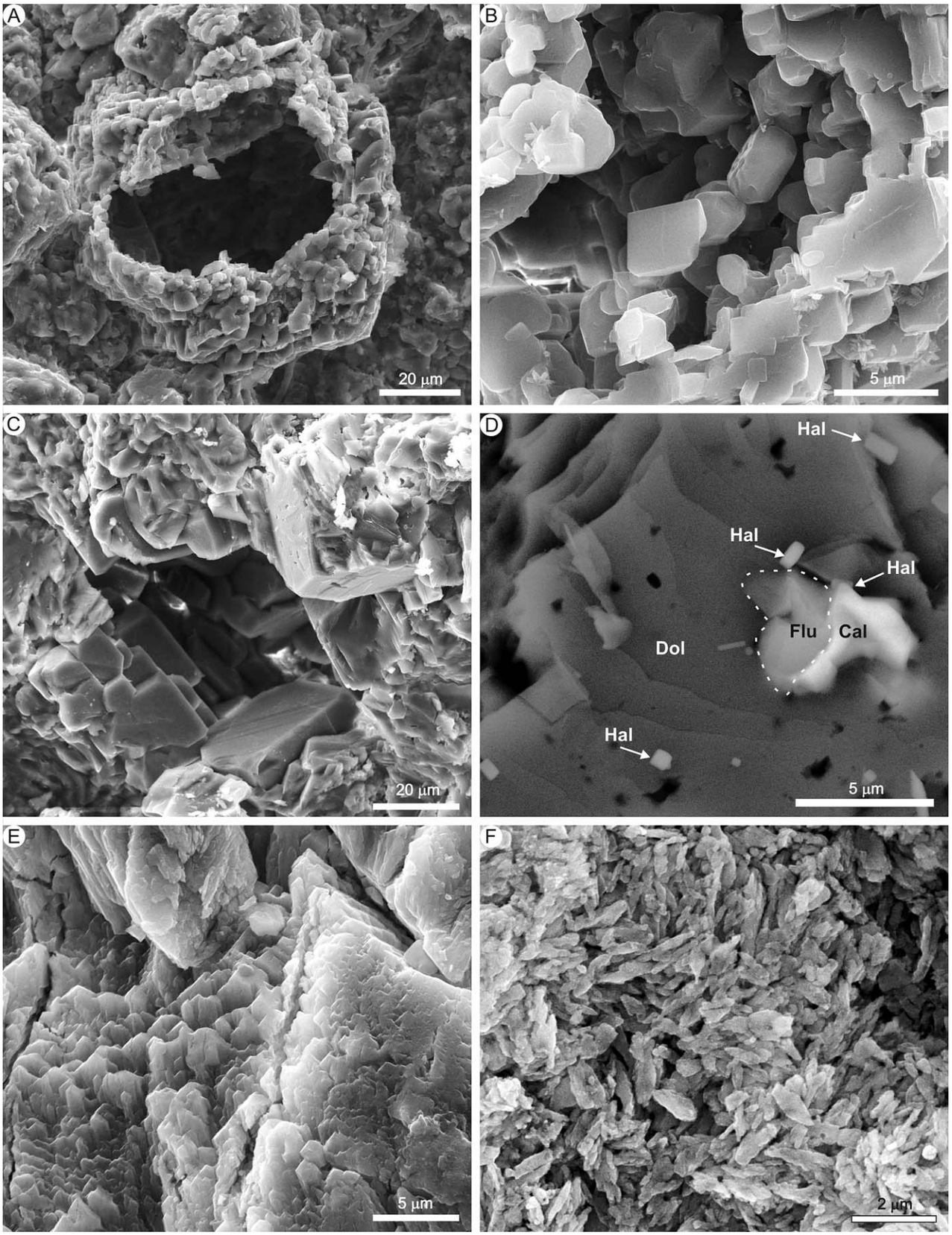
A
20 µm
B
5 µm
C
20 µm
D
Hal
Hal
Hal
Flu
Cal
Dol
Hal
5 µm
E
5 µm
F
2 µm

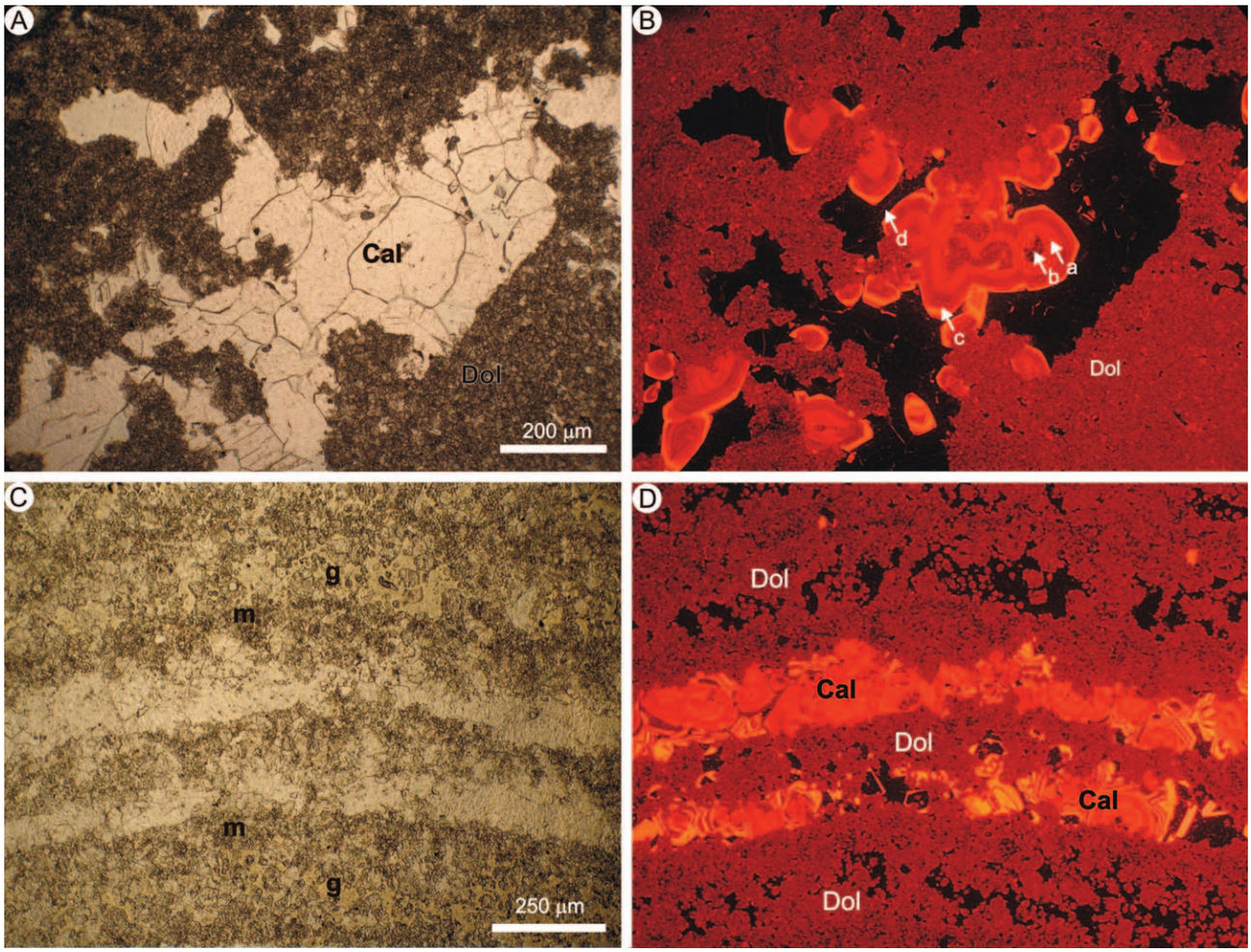

FIG. 7.—Plane-polarized light (left) and the corresponding cathodoluminescence views (right) of Crinkly Bed laminae. Dark areas in the CL pictures are porosity. **A, B)** Mosaic of equant and clear calcite (Cal) crystals that fill secondary cavities after sulfate (as indicated by their shape) in a granular layer of dolomite (Dol). CL view part B reveals that the dolomite is uniformly very dull or nonluminescent (Dol), whereas the coarser sparitic dolomite crystals show a blotchy luminescence. Within the equant crystals of calcite several growth zones of different luminescence color can be distinguished: an early wide, bright orange zone with thin dull subzones (a); a concentric pattern is evident around dark clasts or centers of cementation (b); a much thinner white to orange zone interbedded with dull orange subzones with a more polygonal boundary (c); a dull zone characterizes the outer part of some crystals (d). **C, D)** Alternation of homogeneous micritic darker laminae (m) with granular laminae (g). All dolomite crystals (Dol) are dull luminescent, and detrital laminae in the middle of the picture have been replaced by neomorphic calcite (Cal).

Origin of Dolomite: Primary and Microbial?

The dolomite in Zechstein carbonate traditionally has been interpreted as having resulted from seepage reflux (Clark 1980; Smith 1981; Lee and Harwood 1989). The close association of the Crinkly Bed and adjacent strata with evaporites would be consistent with evaporite-related dolomitization, as in the sabkha model. Moreover, after the deposition of the Roker Formation, additional evaporites were precipitated (the Fordon and Stassfurt evaporites), so that there would have been a further source of potentially dolomitizing fluids. By contrast, several studies have proposed bacterial mediation for the primary precipitation of evaporative Ca dolomite in microbial mats, both in modern environments and in the laboratory (e.g., Vasconcelos et al. 1995; van Lith et al. 2003a; Visscher and Stolz 2005), and the identification of fossilized bacteria in ancient microbial dolomite suggests that these same microbiological processes may explain older dolomite (Garcia del Cura et al. 2001; Rao et al. 2003; van Lith et al. 2003b; Mastandrea et al. 2006; Perri and Tucker 2007; Olivieri et al. 2010). Relicts of early gypsum cement that surround dolomitic grains in the Crinkly Bed laminae indicate prior precipitation of the dolomite, which is very early and synsedimentary. The Crinkly Bed

←

FIG. 6.—SEM microphotographs of fresh surfaces of rock slabs. **A)** Close-up view of a hollow grain composed of micritic crystals of dolomite. **B)** Enlargement of dolomite microcrystals, some of which are subhedral (e.g., in the center of picture). **C)** Subhedral dolomite crystals facing into a small cavity in the center of the picture. **D)** SEM view (back-scattered electron image) of a dolomite crystal interior with inclusions of halite (Hal), fluorite (Flu), and Mg calcite (Cal). Note empty cavities, probably after halite inclusions. **E)** Relicts of subhedral swallow-tail gypsum crystals (close-up view of Fig. 5C). **F)** Microcrystalline gypsum.

TABLE 1.—*Results of XRF analyses of representative bulk samples of the Crinkly Bed. Values in wt%.*

Sample	Na_2O	MgO	Al_2O_3	SiO_2	P_2O_5	K_2O	CaO	TiO_2	MnO	Fe_2O_3	SrO
H1	0.44	36.37	0.12	1.88	0.70	0.02	59.85	0.01	0.07	0.53	0.0070
H2	0.82	36.05	0.20	1.91	0.65	0.04	59.66	0.03	0.07	0.57	0.0077
H3	0.48	35.14	0.39	2.71	0.65	0.05	60.01	0.03	0.10	0.44	0.0076
H4	0.81	34.88	0.56	2.12	0.66	0.08	59.60	0.04	0.12	1.13	0.0060
H5	1.24	33.98	0.33	1.52	0.73	0.05	61.02	0.04	0.16	0.93	0.0060
H6	0.84	31.73	0.38	1.51	0.69	0.05	63.73	0.04	0.11	0.93	0.0068
H7	0.20	19.69	0.32	1.80	0.88	0.04	75.93	0.04	0.10	1.00	0.0081
LP	0.05	36.35	0.18	1.07	0.66	0.03	61.06	0.02	0.08	0.50	0.0055

dolomite, essentially thin laminae of micritic dolomite alternating with thicker laminae of dolomitic peloids, together with the general homogeneous, Ca-rich composition of the dolomite (which is typical of synsedimentary, primary dolomite), suggest a uniform process of dolomite formation.

The $\delta^{18}O$ signature of +1.1 (± 0.3)‰ PDB for the Crinkly Bed dolomite is quite different from other English Zechstein dolomite values (mostly between −1 and −2‰), which fall within the range of the equivalent deposits of Western Europe (Clark 1980; Bechtel and Puttmann 1997). Late Permian seawater is estimated to have had a $\delta^{18}O$ value between 0‰ and −4‰ SMOW (Veizer et al. 1997). Thus, with the characteristic fractionation effect of dolomite relative to co-precipitating $CaCO_3$, positive $\delta^{18}O$ values for the dolomite would be consistent with precipitation from seawater. The positive values of the dolomite also suggest that there has been little resetting of the isotope signatures through later recrystallization. The dull-luminescent nature of the early dolomite, typical of a marine precipitate with no Mn present, is consistent with this interpretation.

The very high positive $\delta^{13}C$ signature (+6.9‰ ± 0.3‰) for the Crinkly Bed dolomite is typical for Permian marine carbonate (Veizer et al. 1999), and contrasts with 0.1–1.7‰ $\delta^{13}C$ of Abu Dhabi primary dolomite. The supposed more typical, quite negative $\delta^{13}C$ values for microbial precipitates (e.g., Schidlowski 2000) are not present in the Crinkly Bed, but then normal-marine $\delta^{13}C$ values are common for microbialites (Andres et al. 2006), and is thus not inconsistent with a microbial origin.

The small size of the micritic crystals in the Crinkly Bed, the excess of Ca and lack of Fe and Mn, plus the $\delta^{18}O$ values, suggest very early formation of the dolomite, so that a primary biotic origin of the dolomite in both the micritic laminae and the autochthonous peloidal laminae is strongly advocated. The presence of microbial fossils in the Crinkly Bed laminae is also consistent with such an origin (cf. Perri and Tucker 2007).

Origin of Centimeter Scale Crinkly Bed Structures: Microbially Induced Sedimentary Structures

The lamination and morphologies of microbial mats in peritidal carbonate environments are quite variable (Alsharhan and Kendall 2003). With the Crinkly Bed, the variation from ripple-like macrostructures through to domal–conical stromatolites likely reflects a complex interaction between microbial processes and physical processes of current and wave action.

Primary physical sedimentary structures form by physical processes of erosion, transportation, and deposition of grains, and their later deformation. They usually have been separated from biogenic sedimentary structures, such as stromatolites, which are characterized by positive (strongly convex upward, beyond the angle of repose) growth structures because of the role of microorganisms. However, microorganisms can modify sedimentary structures without producing marked primary relief. These microbially mediated structures, forming in both siliciclastic and carbonate systems, and resulting from the interaction between epibenthic

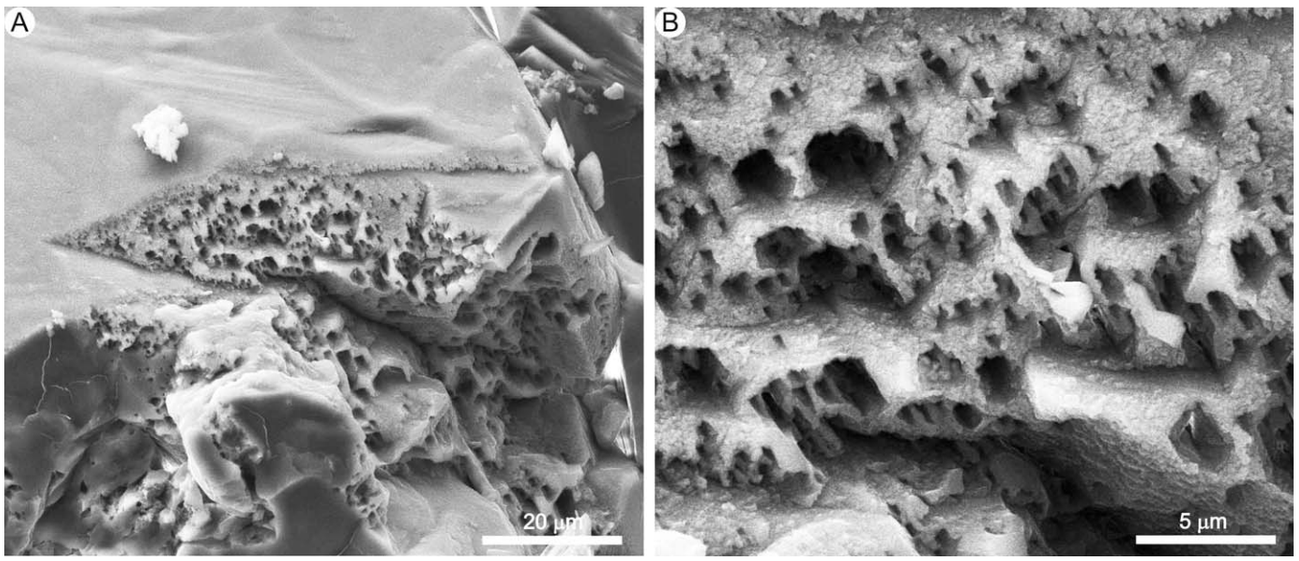

FIG. 8.—SEM images of a fresh surface. **A)** Secondary calcite crystals at the interface with dolomite or gypsum crystals. **B)** Close-up view of part A showing elongate and polygonal microcavities characterizing the surface, and the granular nanotexture of the mineral itself, consisting of coalescing spheroidal to irregular nanocrystals.

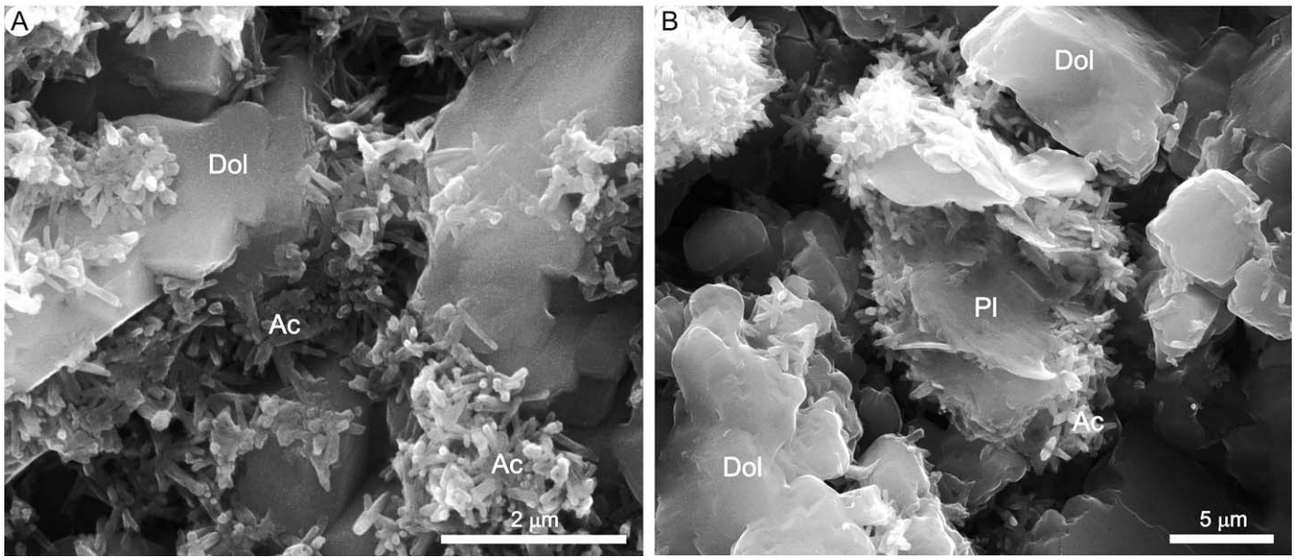

FIG. 9.—SEM views (fresh surfaces) of crystal aggregates of Fe/Mn oxides or hydroxides (acicular crystals, Ac) and (Fe, Mg, Al) silicate minerals (platy crystals, Pl, in part B), among dolomitic crystals (Dol).

bacterial–microbial communities with physical processes, have been referred to as *microbially induced sedimentary structures*, MISS, by Gerdes et al. (2000) and Noffke et al. (2001). These MISSs may form in association with physical sedimentary processes but where ecological conditions are favorable for biofilms and microbial mats to cover the sediment surface. One feature of MISSs is that sediment is stabilized by the mats, and thus is more resistant to erosion (Noffke 1998, 1999). Baffling, trapping, and binding of grains by subvertically oriented filamentous cyanobacteria can lead to an alternation of organic-rich and grain-rich laminae, as in stromatolites, which are also referred to as *biolaminites* (Noffke and Krumbein 1999).

In the case of the Crinkly Bed, the ripple-like macrostructures on two scales, showing complex crest patterns, and interference patterns, are similar to wave–current processes that produce ladderback and other ripple types on a tidal flat or in the shallow subtidal (Reddering 1987; Fraser et al. 1991). However, as described earlier, the Crinkly Bed has a lamination typical of microbialites—the alternation of micritic and granular laminae, consistent thickness, lateral persistence of laminae for several meters, a decimeter-scale thickness of the undulations and crinkles of the lamination topography, and a lack of cross lamination. In addition, the grainy laminae are composed chiefly of peloids, which we interpret as having formed *in situ* through microbial processes, with few detrital grains. If all this is so, the lamination reflects a biofilm covering the sediment surface, in which case the ripple-like structures are not simply the result of the interaction of waves and currents with loose sediment grains.

There are several possible explanations for the ripple-like macrostructures, of which inheritance of ripple bedforms, or deformation of a biofilm, are the most likely. It could be that loose, mobile, granular sediment was transported and deposited in the form of ripple bedforms, and then this undulating layer acted as a template that was covered with a laterally persistent, isopachous biofilm, which maintained the original pattern of the ripples up through several decimeters of strata. This explanation would account for the isopachous and microbial origin of the lamination of the ripple-like macrostructures. However, rippled units of peloidal grainstone–packstone or individual rippled lenses have not been observed in the 1.4-meter-thick section of the Crinkly Bed. In spite of good outcrops, it may be a question of the critical evidence not being exposed. If these features formed by deformation of a surficial biofilm, it could be the result of several processes: downslope movement of the surficial microbial mat, disturbance through gas or water escape, or the effect of the physical action of waves and currents deforming the mat into undulations. There is no evidence for larger-scale slumping in the Crinkly Bed or units above and below, nor for any breakup of the lamination due to significant horizontal movement. There are no intraclastic breccias present either, on the scale that would be expected if mass movement were

TABLE 2.—*Stable-isotope measurements of representative dolomite samples of the Boulder Conglomerate and Crinkly Bed laminites and calcite cement.*

	DOLOMITE			CALCITE		
Sample	%	$\delta^{13}C$ (PDB), ‰	$\delta^{18}O$ (PDB), ‰	%	$\delta^{13}C$ (PDB), ‰	$\delta^{18}O$ (PDB), ‰
H1	96	6.55	0.68	-	-	-
H2	96	6.80	1.06	-	-	-
H3	93	6.94	1.41	2	-	-
H4	93	6.83	1.19	2	-	-
H5	90	7.15	1.31	5	-	-
H6	84	5.08	0.29	11	-	-
H7	53	6.10	0.89	43	−4.04	−4.92
LP	96	7.10	1.08	1	-	-
CA	-	-	-	100	−7.44	−6.18

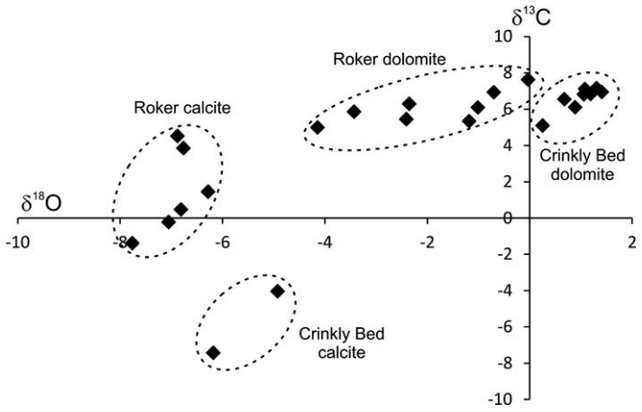

FIG. 10.—Isotope data for dolomite and calcite from the Crinkly Bed, presented in Table 2, compared with data for dolomite (8 values, average = −1.91‰ for $\delta^{18}O$ and 6.06‰ for $\delta^{13}C$) and calcite (dedolomite, 6 values, average = −6.9‰ for $\delta^{18}O$ and 1.44‰ for $\delta^{13}C$) from the Roker Fm at outcrop, NE England (data from Clark 1980).

involved. With deposition in a lagoonal environment, with no likely gradient, lateral movement of mat-stabilized sediment would not be expected. Gas or water escape would result in deformation of the microbial mat, but this would be expected to lead to disruption, fracturing, and contortion of the lamination, which is not seen. The remarkably persistent, isopachous nature of the lamination is a distinctive feature of this unit.

The domal–conical structures are typical microbial-growth structures, but these were likely in some cases still affected by currents, as suggested by their asymmetry. These features are not unlike the Monroe structures recorded on muddy tidal flats ascribed to dewatering, although they are apparently typical of cold climates (Dionne 1973). However, the lamination in the Crinkly Bed is mainly isopachous and continuous, as it is in these conical structures, with no disruptions, so that a dewatering origin is ruled out.

Deformation of a surficial biofilm by waves and currents during the growth of the biofilm could produce the ripple-like macrostructures, particularly if the biofilm was coherent. The larger structures with a common north–south crest orientation would reflect stronger waves or currents parallel to the basin margin shoreline; the smaller-scale symmetrical ripple-like structures would reflect weaker wave action. Deformation of the biofilm at this 1–10 cm scale could have led to the generation of the asymmetric, curved-crested features with steep sides. The lack of *in situ* brecciation of the laminae suggests that synsedimentary lithification was not taking place, and intraclasts are not abundant.

Processes of lithification of modern mats range from completely microbial to purely chemically mediated mechanisms. Two major factors determine the extent of precipitation: the environmental control on organic-matter decomposition (mainly EPS), and the saturation state of the solution with respect to carbonate minerals, which depends on the ion-activity product, solubility product, and pH (Dupraz and Visscher 2005). In modern, normal-marine, stromatolite-producing mats, local environmental conditions cause the communities to turn over within the mats, producing alternating thin micritic and cemented granular laminae (Reid et al. 2000). Cement precipitation and lithification are inhibited by low biomass (Dupraz and Visscher 2005). Such microbial mats can renew annually and grow through to trap and bind sediment, with little carbonate precipitation. These conditions favor the biostabilization of the sediment surface and formation of microbially induced sedimentary structures.

In the case of the Crinkly Bed lamination, with an *in situ* origin of the peloidal grains and the apparent near-absence of allochthonous grains, extensive cementation of the biofilm close to, or just below, the seafloor does not seem to have taken place, since intraclasts are rare. Rather, the biofilm remained cohesive at, and just below, the surface, and it was resistant to erosion, before cementation some distance below by gypsum.

Overall, the features of the Crinkly Bed indicate deposition in a shallow subtidal environment, in water depth of several meters, where the seafloor was covered by a biofilm. The formation of the ripple-like structures is unclear, however: they could be inherited structures from earlier ripples, for which there is no evidence, or they could have been generated by deformation of the surficial microbial mat through wave or current action. Some degree of hypersalinity was likely, in view of the absence of higher organisms and the presence of early gypsum cement.

Origin of Coniform Stromatolitic Structures

Throughout the fossil record, but particularly in the Proterozoic, cone-shaped stromatolites (e.g., *Conophyton* Maslov) are distributed widely and range in height from a few centimeters to several meters (Riding and Awramik 2000). Their origin, inferred from modern counterparts, is a response of either chemotactic or phototactic gliding of microorganisms, which are mostly filamentous cyanobacteria (Golubic et al. 2000). Fossil coniforms have often been interpreted as microbial, even if, as with Archean cases, there is the possibility of an abiotic origin (Grotzinger and Rothman 1996; MacLoughlin et al. 2008). Their biogenicity seems to be convincing considering the environmental context and the morphology of the lamination (Allwood et al. 2006). Crinkly Bed coniforms closely resemble the Archean forms (Hofmann et al. 1999). The biotic origin of the Crinkly Bed lamination is confirmed by the absence of abundant cements, and the presence of autochthonous grains and fossil microbial filaments, including subvertical fossil filaments (Fig. 11B), which could testify to the upward growth of a phototactic biofilm.

Grotzinger and Rothman (1996) and Batchelor et al. (2004) proposed biotic models for stromatolite morphogenesis that considers the relationship between upward growth of a phototropic or phototactic biofilm and mineral precipitation normal to the surface. Following this conceptual model, coniform structures with thickened apical zones form when localized upward growth of the biofilm is greater than lateral accretion, whereas more angular coniform structures develop where vertical microbial growth prevails over the whole structure.

In the Crinkly Bed, some larger cones on the surface have a bulge around their base (Fig. 12C), suggesting soft-sediment flexure of the laminae during minor downslope movement (similar to Archean coniforms of Australia, Allwood et al. 2006, their fig. 21 suppl. mat.). The nipple-like projection of the Crinkly Bed cones could similarly represent a symmetrical collapse of the peak and a new phase of growth (Fig. 12C), or a break in the development of the microbial community in favor of more detrital accumulation, with some erosion and then subsequent regrowth (e in Fig. 12C).

Depositional Context of the Crinkly Bed and Associated Strata

As described earlier, the Crinkly Bed was deposited in an elongate lagoon, at least 1.5 km wide and more than 10 km long, located behind the former reef crest, within and upon the back-reef area, of the previously deposited Ford Formation. The microbial Crinkly Bed followed a stratigraphic hiatus after deposition of the Boulder Conglomerate and Hartlepool Anhydrite. The upward transition from the Crinkly Bed into overlying large microbial domical buildups and grainstone units suggests an overall increase in accommodation space (relative rise of sea level) and is therefore interpreted as the transgressive systems tract. The increasingly oolitic grainstone of the upper part of the overlying Roker Formation is interpreted as the succeeding highstand of this third

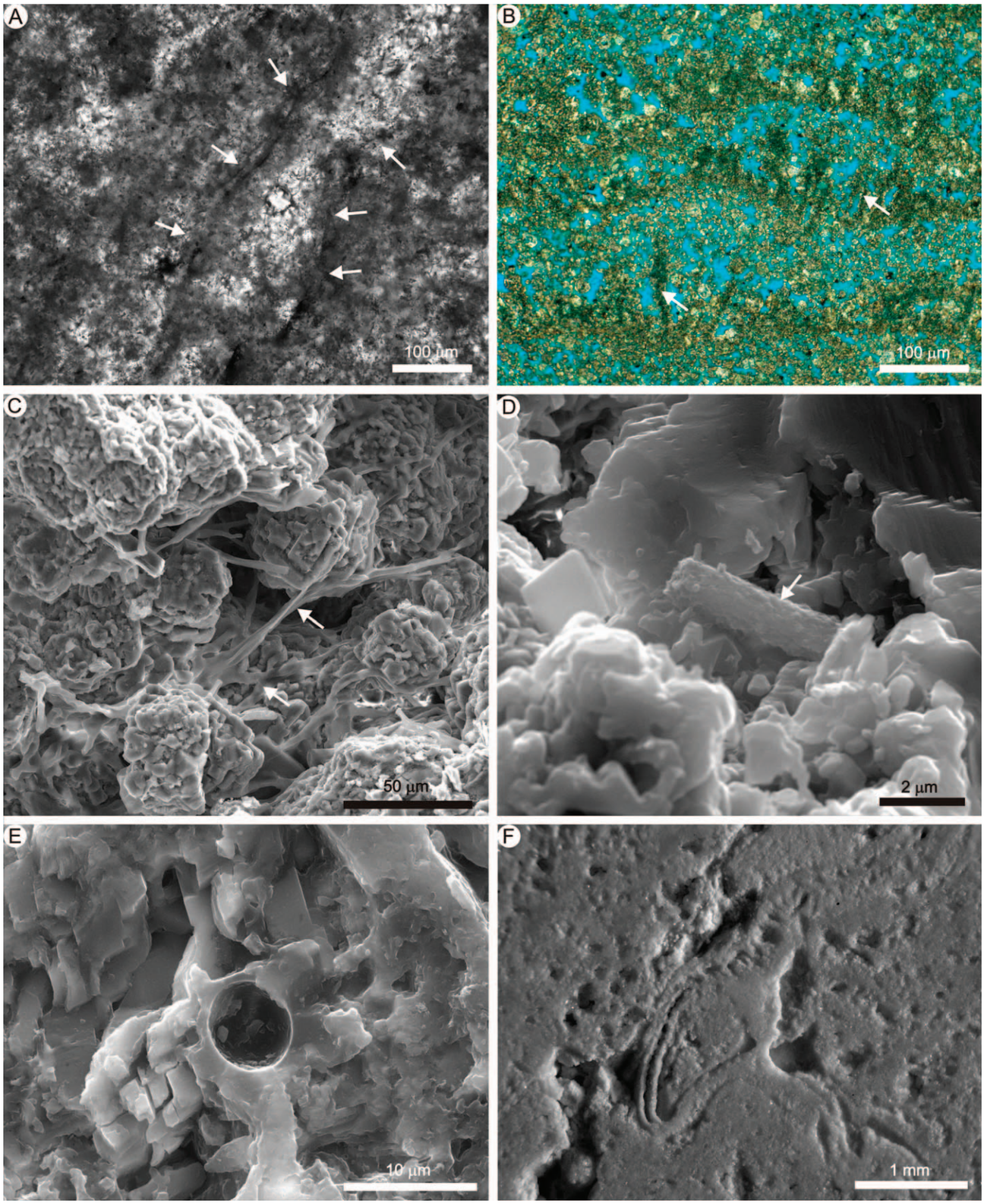

FIG. 11.—Relics of microfossil forms in Crinkly Bed laminae (A and B are photomicrographs, C–E are SEM images of fresh surfaces, and F is a polished slab). **A)** Nonseptate subspherical tubes (white arrows) along homogeneous micritic laminae. **B)** Micritized filaments with a fan-like subvertical trend, originating from micritic laminae. Porosity is blue areas. **C)** Interpreted remains of filamentous organic matter. **D)** Single phosphate-rich (apatite?) cyanobacteria-like filament (arrowed). **E)** Empty mold of coccoid form. **F)** Tubes that cut across laminae.

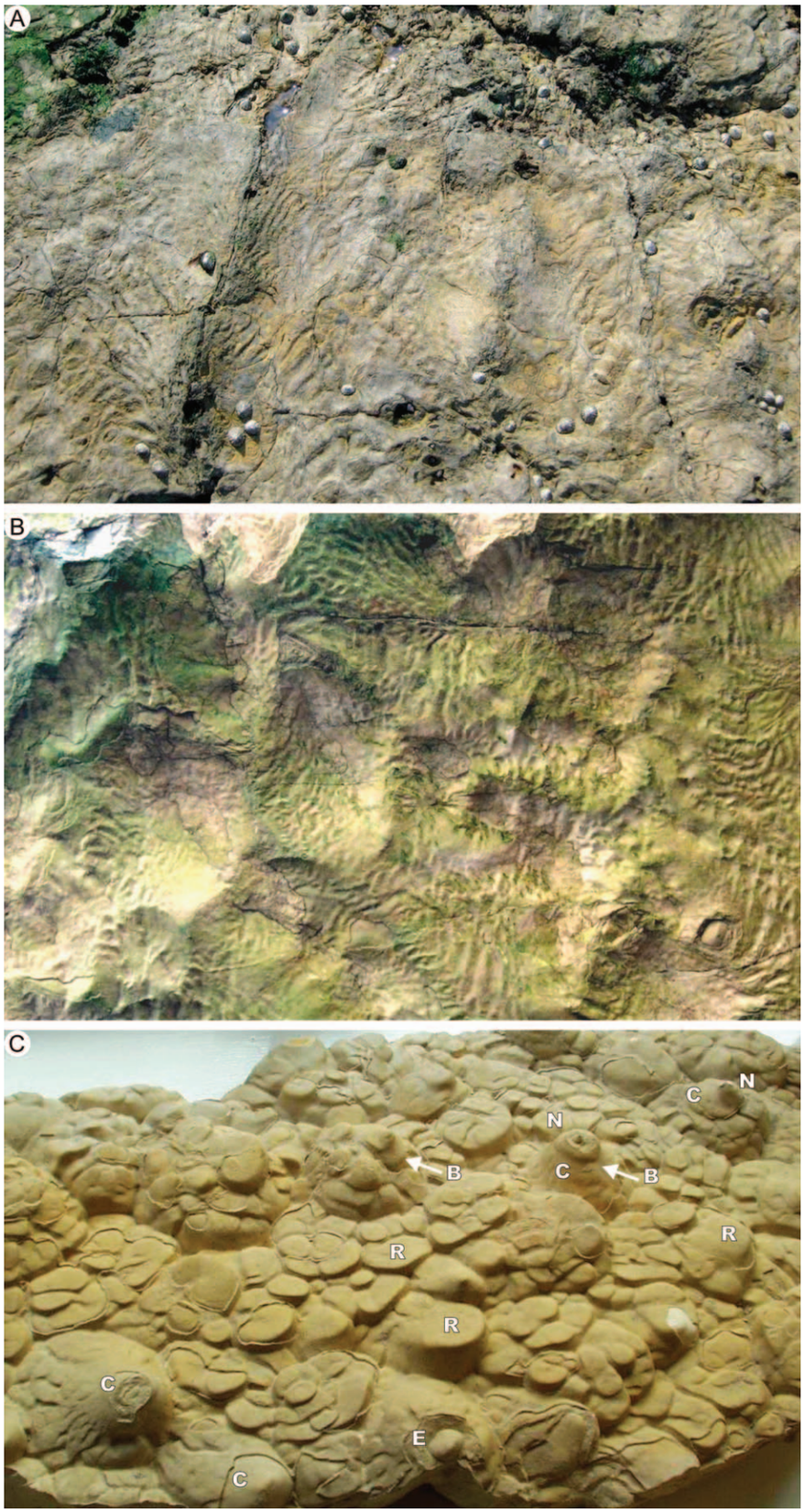

FIG. 12.—Crinkly Bed sedimentary macrostructures. **A)** Ripple-like forms on bedding surface (with limpets) showing two scales: larger with straight to ellipsoidal crests and centimeter scale smaller structures with complex patterns of crest orientation (field of view 1.0 m × 1.5 m) Foreshore, Blackhall Rocks, Co. Durham. **B)** Ripple-like structures on roof of cave (underside of bed) with complex crest pattern of small-scale ripple-like structures superimposed on larger-scale ellipsoidal to domical structures (field of view 1.0 m × 1.25 m). The Gin Cave, Blackhall Rocks, Co. Durham. **C)** Slab, from Hawthorn Quarry, Co. Durham,) shows a variety structures: curvilinear–cuspate structures (R), some with nearly vertical steep sides. Others are conical–domal structures (C) with nipple-like tops (N) and bulges of the lower part (B) or with an erosional surface (E) with subsequent regrowth of a small cone. Inferred palaeocurrent from top left to bottom right.

Zechstein sequence (ZS3, Tucker 1991). The lateral, basinward equivalent of the Crinkly Bed, interbedded dolomite and evaporite deposits, indicates that salinity was probably quite high during deposition of the Crinkly Bed itself, which is also supported by its gypsum cementation and replacement. This lagoon then became more open as sea level continued to rise, and led to the deposition of the low domical mounds and oolites under a higher-energy regime.

Crinkly Bed Diagenesis and Bacterial Sulfate Reduction

The general diagenetic history of the Crinkly Bed reflects the various stages already documented for Zechstein carbonate (Tucker and Hollingworth 1986; Hollingworth and Tucker 1987; Lee and Harwood 1989). Marine cements appear to have been rare, although micritic laminae may contain marine cements, but this is impossible to confirm. Vadose compaction textures in the grainstone above the Crinkly Bed suggest early exposure to meteoric fluids (Clark 1980). Later burial precipitation of dolomite in the Crinkly Bed is suggested by the presence of large (several 100 μm) dolomite spar crystals filling primary pore space (Fig. 6C). Their lower Ca content, excess Mg, and low Fe, as compared to the micritic dolomite, is consistent with a burial origin.

During uplift from early Cretaceous through early Tertiary, the Zechstein dolomite was affected by extensive meteoric diagenesis that dissolved the evaporite bodies (Tucker and Hollingworth 1986; Braithwaite 1988). The dissolution of the evaporites resulted in the calcitization of dolomite (dedolomitization) and precipitation of calcite cements, as well as in the formation of collapse breccias and evaporite residues. In the Crinkly Bed and Roker Formation generally, the occurrence of coarse calcite, which replaced both dolomite and gypsum, and its presence in cavities and vugs is consistent with a late, telogenetic origin related to evaporite dissolution. A meteoric origin for this late calcite is confirmed by negative $\delta^{18}O$ (−6.2, −4.9‰) and $\delta^{13}C$ values (−7.4, −4.0‰), even though the $\delta^{13}C$ values are even more negative than other late calcite cements in the Zechstein domain (Fig. 10). Such negative values of $\delta^{13}C$ would be consistent with a microbially mediated origin of the late calcite, possibly as a consequence of bacterial sulfate reduction (BSR) that induced an increase in alkalinity and resulted in precipitation of carbonate minerals. Calcite, aragonite, and dolomite have all been reported as precipitated through BSR (Pierre and Rouchy 1988; Anadón et al. 1992; Peckmann et al. 1999; Machel 2001; Ziegenbalg et al. 2010). Gypsum dissolution could have furnished the SO_4^{2-} ions that SRB use as an electron acceptor during anaerobic oxidation of residual organic matter. The microcavities produced by gypsum replacement and the nanostructure of aggregates of calcite nanoparticles in this late calcite, described earlier, support the replacement of sulfate minerals as a key process, and suggest a microbial origin for this calcite. Calcite consisting of an aggregation of mineral nanoparticles (nonclassical crystallization of Niederberger and Cölfen 2006) has been recognized as a common biosignature of modern and ancient microbial carbonate (Lopez-Garcia et al. 2005; Benzerara et al. 2006; Perri and Tucker 2007; Bontognali et al. 2008; Sánchez-Román et al. 2008; Benzerara et al. 2010; Manzo et al. 2012; Perri and Spadafora 2011; Perri et al. 2012a; Perri et al. 2012b).

CONCLUSIONS

The Crinkly Bed a distinctive 1.4-meter-thick stromatolite unit (northeastern England, Upper Permian Zechstein succession, Z2C) was deposited in an elongate lagoon, at least 1.5 km wide and more than 10 km long, located behind the former reef crest of the previously deposited Ford Formation (upper part of Zechsteinkalk, Z1C), following a major phase of subaerial exposure, when evaporites were deposited in the basin to the east. The lagoon floor was colonized by a microbial mat, which, in high-salinity conditions, led to the microbially mediated precipitation of primary micritic dolomite which as clotted peloidal to aphanitic layers alternating with layers of autochthonous, silt-size granular peloids, creating a distinctive millimeter-scale lamination. Few allochthonous grains, mostly calcispheres, and evaporite crystals were also incorporated in the deposits.

The Crinkly Bed shows macrostructures that vary from centimeter scale, ripple-like features (of varied orientation and geometry) to domal and conical stromatolitic microbially controlled structures. The origin of the ripple-like features is equivocal, with two likely interpretations: inheritance of the ripple-like forms from wave-rippled granular bedforms, although there is no evidence for the original ripples, and deformation of the thin surficial biofilm or microbial mat by the physical action of waves and currents, during deposition in water depths of several meters. The evidence is also equivocal as to whether the microbial mat was being cemented on the seafloor or was simply cohesive.

Gypsum cement was precipitated between the grains during early diagenesis, while dissolution features suggest later exposure to meteoric fluids. A burial diagenetic phase is evidenced by the formation of ferroan sparry dolomite, whereas uplift in the Tertiary and consequent meteoric exposure caused precipitation of calcite cements that replaced gypsum and pre-existing dolomite (mainly grains), probably via sulfate-reducing bacteria that oxidized residual organic compounds.

Examination of the Crinkly Bed shows that it is the result of synsedimentary and postsedimentary physical *and* microbially mediated processes that generated a complicated deposit in which it has been possible, using a multi-scale approach of investigation, to develop a model to track the evolution of a carbonate unit formed in an evaporitic context, like the Pre-Salt microbial carbonates of the South Atlantic basins. Such sedimentary environments (marine or continental) provide ideal conditions for the development of microbial communities, and thus microbial carbonates, which may form before and during evaporite precipitation. Microbes also play a fundamental role in carbonate dissolution, precipitation, and replacement from early through to late diagenesis. The synsedimentary and postsedimentary interaction of evaporites and carbonates lead to complicated patterns of evolution including the mixing of biotic and abiotic processes, making the interpretation of the final deposit often very difficult.

ACKNOWLEDGMENTS

The authors are extremely grateful to two anonymous reviewers, Associate Editor Paul Myrow, Rob Riding, and Editor Gene Rankey for all their detailed comments and thoughtful suggestions on this paper, which have improved the interpretations considerably. Neville Hollingworth collected the slab featured in Figure 12C.

REFERENCES

Allwood, A.C., Walter, M.R., Kamber, B.S., Marshall, C.P., and Burch, I.W., 2006, Stromatolite reef from the Early Archaean era of Australia: Nature, v. 441, p. 714–718.

Alsharhan, A.S., and Kendall, C.G.St.C., 2003, Holocene coastal carbonates and evaporites of the southern Arabian Gulf and their ancient analogues: Earth-Science Reviews, v. 61, p. 191–243.

Anadón, P., Rosell, L., and Talbot, M.R., 1992, Carbonate replacement of lacustrine gypsum deposits in two Neogene continental basins, eastern Spain: Sedimentary Geology, v. 78, p. 201–216.

Andres, M.S., and Reid, R.P., 2006, Growth morphologies of modern marine stromatolites: a case study from Highborne Cay, Bahamas: Sedimentary Geology, v. 185, p. 319–328.

Andres, M.S., Sumner, D.Y., Reid, R.P., and Swart, P.K., 2006, Isotopic fingerprints of microbial respiration in aragonite from Bahamian stromatolites: Geology, v. 34, p. 973–976.

Awramik, S., 2006, Respect for stromatolites: Nature, v. 441, p. 700–701.

Awramik, S.M., and Riding, R., 1988, Role of algal eukaryotes in subtidal columnar stromatolite formation: National Academy of Science (USA), Proceedings, v. 85, p. 1327–1329.

Batchelor, M.T., Burne, R.V., Henry, B.I., and Jackson, M.J., 2004, A case for biotic morphogenesis of coniform stromatolites: Physica A, Statistical Mechanics and its Applications, v. 337, p. 319–326.

Bechtel, A., and Püttmann, W., 1997, Palaeoceanography of the early Zechstein Sea during Kupferschiefer deposition in the Lower Rhine Basin (Germany): a reappraisal from stable isotope and organic geochemical investigations: Palaeogeography, Palaeoclimatology, Palaeoecology, v. 136, p. 331–358.

Benzerara, K., Menguy, N., Lopez-Garcia, P., Yoon, T.H., Kaźmierczak, J., Tyliszczak, T., Guyot, F., and Brown, G.E., Jr., 2006, Nanoscale detection of organic signatures in carbonate microbialites: National Academy of Science (USA), Proceedings, v. 103, p. 9440–9445.

Benzerara, K., Meibom, A., Gautier, Q., Kaźmierczak, J., Stolarski, J., Menguy, N., and Brown, G.E., Jr., 2010, Nanotextures of aragonite in stromatolites from the quasi-marine Satonda crater lake, Indonesia, *in* Pedley, H.M., and Rogerson, M., eds., Tufas and Speleothems: Unravelling the Microbial and Physical Controls: Geological Society of London, Special Publication 336, p. 211–224.

Bontognali, T.R.R., Vasconcelos, C., Warthmann, R.J., Dupraz, C., Bernasconi, S., and McKenzie, J.A., 2008, Microbes produce nanobacteria-like structures, avoiding cell entombment: Geology, v. 36, p. 663–666.

Bontognali, T., Vasconcelos, C., Warthmann, R.J., Bernasconi, S., Dupraz, C., Strohmenger, C.J., and McKenzie, J.A., 2010, Dolomite formation within microbial mats in the coastal sabkha of Abu Dhabi (United Arab Emirates): Sedimentology, v. 57, p. 824–844.

Braithwaite, C.J.R., 1988, Calcitization and compaction in the Upper Permian Concretionary Limestone and Seaham Formations of North-East England: Yorkshire Geological Society, Proceedings, v. 47, p. 33–45.

Brasier, A.T., Andrews, J.E., and Kendall, C.G.St.C., 2011, Diagenesis or dire genesis? The origin of columnar spar in tufa stromatolites of central Greece and the role of chironomid larvae: Sedimentology, v. 58, p. 1283–1302.

Castanier, S., Le métayer-Levrel, G., and Perthuisot, J.P., 2000, Bacterial roles in the precipitation of carbonate minerals, *in* Riding, R.E., and Awramik, S.M., Microbial Sediments: Berlin, Springer, p. 32–39.

Clark, D.N., 1980, The diagenesis of Zechstein carbonate sediments: Contributions to Sedimentology, v. 9, p. 167–203.

Dionne, J.C., 1973, Monroes: a type of so-called mud volcano in tidal flats: Journal of Sedimentary Petrology, v. 43, p. 848–856.

Dupraz, C., and Visscher, P.T., 2005, Microbial lithification in marine stromatolites and hypersaline mats: Trends in Microbiology, v. 13, p. 429–438.

Dupraz, C., Visscher, P.T., Baumgartner, L.K., and Reid, R.P., 2004, Microbe–mineral interactions: early carbonate precipitation in a hypersaline lake (Eleuthera Island, Bahamas): Sedimentology, v. 51, p. 745–765.

Dupraz, C., Reid, R.P., Braissant, O., Decho, A.W., Norman, R.S., and Visscher, P.T., 2009, Processes of carbonate precipitation in modern microbial mats: Earth-Science Reviews, v. 96, p. 141–162.

Fraser, G.S., Thompson, T.A., Kvale, E.P., Carlson, C.P., Fishbaugh, D.A., Gruver, B.L., Holbrook, J., Kairo, S., Kohler, C.S., Malone, A.E., Moore, C.H., Rachmanto, B., and Rhoades, L., 1991, Sediments and sedimentary structures of a barred, non-tidal coastline, southern shore of Lake Michigan: Journal of Coastal Research, v. 7, p. 1113–1124.

García del Cura, M.A., Calvo, J.P., Ordóñez, S., Jones, B.F., and Cañaveras, J.C., 2001, Petrographic and geochemical evidence for the formation of primary, bacterially-induced lacustrine dolomite: La Roda "white earth" (Pliocene, central Spain): Sedimentology, v. 48, p. 897–915.

Gerdes, G., Klenke, T., And Noffke, N., 2000, Microbial signatures in peritidal siliciclastic sediments: a catalogue: Sedimentology, v. 47, p. 279–308.

Golubic, S., Seong-Joo, L., and Browne, K.M., 2000, Cyanobacteria: architects of sedimentary structures, *in* Riding, R.E., and Awramik, S.M., eds., Microbial Sediments: Berlin, Springer, p. 57–67.

Grotzinger, J.P., and Rothman, D.H., 1996, An abiotic model for stromatolite morphogenesis: Nature, v. 383, p. 423–425.

Harwood, G.M., Smith, D.B., Lee, M.R., and Kendall, A.C., 1990, Carbonate–evaporite sedimentation in the Zechstein Basin, field excursion guidebook: International Association of Sedimentologists, Congress, August, Nottingham.

Hofmann, H.J., Grey, K., Hickman, A.H., and Thorpe, R.I., 1999, Origin of 3.45 Ga coniform stromatolites in Warrawoona Group, Western Australia: Geological Society of America, Bulletin, v. 111, p. 1256–1262.

Hollingworth, N.T.J., and Tucker, M.E., 1987, The Upper Permian (Zechstein) Tunstall Reef of northeast England: palaeoecology and early diagenesis, *in* Peryt, T.M., ed., The Zechstein Facies in Europe: Berlin, Springer-Verlag, p. 23–50.

Konhauser, K., 2007, Introduction to Geomicrobiology: Blackwell Science, Oxford, U.K., 425 p.

Lee, M.R., and Harwood, G.M., 1989, Dolomite calcitization and cement zonation related to uplift of the Raisby Formation (Zechstein carbonate), northeast England: Sedimentary Geology, v. 65, p. 285–305.

López-García, P., Kaźmierczak, J., Benzerara, K., Kempe, S., Guyot, F., and Moreira, D., 2005, Bacterial diversity and carbonate precipitation in the giant microbialites from the highly alkaline Lake Van, Turkey: Extremophiles, v. 9, p. 263–274.

Machel, H.G., 2001, Bacterial and thermochemical sulfate reduction in diagenetic settings: old and new insights: Sedimentary Geology, v. 140, p. 143–175.

MacLoughlin, N., Wilson, L.A., and Brasier, M.D., 2008, Growth of synthetic stromatolites and wrinkle structures in the absence of microbes: implications for the early fossil record: Geobiology, v. 6, p. 95–105.

Manzo, E., Perri, E., and Tucker, M.E., 2012, Carbonate deposition in a fluvial tufa system: processes and products (Corvino Valley, Southern Italy): Sedimentology, v. 59, p. 553–577.

Mastandrea, A., Perri, E., Russo, F., Spadafora, A., and Tucker, M.E., 2006, Microbial primary dolomite from a Norian carbonate platform: northern Calabria, southern Italy: Sedimentology, v. 53, p. 465–480.

Mawson, M., and Tucker, M.E., 2009, High-frequency cyclicity (Milankovitch and millennial-scale) in slope-apron carbonates: Zechstein (Upper Permian), North-east England: Sedimentology, v. 56, p. 1905–1936.

McKenzie, J.A., 1981, Holocene dolomitization of calcium carbonate sediments from the coastal sabkhas of Abu Dhabi, UAE: a stable isotope study: Journal of Geology, v. 89, p. 185–198.

McKenzie, J.A., and Vasconcelos, C., 2009, Dolomite Mountains and the origin of the dolomite rock of which they mainly consist: historical developments and new perspectives: Sedimentology, v. 56, p. 205–219.

Niederberger, M., and Colfen, H., 2006, Oriented attachment and mesocrystals: Non-classical crystallization mechanisms based on nanoparticle assembly: Physical Chemistry Chemical Physics, v. 8, p. 3271–3287.

Noffke, N., 1998, Multidirected ripple marks rising from biological and sedimentological processes in modern lower supratidal deposits (Mellum Island, southern North Sea): Geology, v. 26, p. 879–882.

Noffke, N., 1999, Erosional remnants and pockets evolving from biotic–physical interactions in a Recent lower supratidal environment: Sedimentary Geology, v. 123, p. 175–181.

Noffke, N., and Krumbein, W.E., 1999, A quantitative approach to sedimentary surface structures contoured by the interplay of microbial colonization and physical dynamics: Sedimentology, v. 46, p. 417–426.

Noffke, N., Gerdes, G., Klenke, T., and Krumbein, W.E., 2001, Microbially induced sedimentary structures: a new category within the classification of primary sedimentary structures: Journal of Sedimentary Research, v. 71, p. 649–656.

Oliveri, E., Neri, R., Ballanca, A., and Riding, R., 2010, Carbonate stromatolites from a Messinian hypersaline setting in the Caltanissetta Basin, Sicily: petrographic evidence of microbial activity and related stable isotope and rare earth element signatures: Sedimentology, v. 57, p. 142–161.

Peckmann, J., Paul, J., and Thiel, V., 1999, Bacterially mediated formation of diagenetic aragonite and native sulfur in Zechstein carbonates (Upper Permian, Central Germany): Sedimentary Geology, v. 126, p. 205–222.

Perri, E., and Spadafora, A., 2011, Evidence of microbial biomineralization in modern and ancient stromatolites, *in* Seckbach, J., and Tewari, V., eds., The Stromatolites: Interaction of Microbes with Sediments. Cellular Origin, Life in Extreme Habitats and Astrobiology: Berlin, Springer-Verlag, v. 18, p. 631–649.

Perri, E., and Tucker, M.E., 2007, Bacterial fossils and microbial dolomite in Triassic stromatolites: Geology, v. 35, p. 207–210.

Perri, E., Manzo, E., and Tucker, M.E., 2012a, Multi-scale study of the role of the biofilm in the formation of minerals and fabrics in calcareous tufa: Sedimentary Geology, v. 263–264, p. 16–29.

Perri, E., Tucker, M.E., and Spadafora, A., 2012b, Carbonate organo-mineral micro- and ultra-structures in sub-fossil stromatolites: Marion Lake, South Australia: Geobiology, v. 10, p. 105–117.

Pierre, C., and Rouchy, J.M., 1988, Carbonate replacements after sulfate evaporites in the middle Miocene of Egypt: Journal of Sedimentary Petrology, v. 58, p. 446–456.

Pope, M., Grotzinger, J.P., and Schreiber, B.C., 2000, Evaporitic subtidal stromatolites produced by *in situ* precipitation: textures, facies association, and temporal significance: Journal of Sedimentary Research, v. 70, p. 1139–1151.

Rao, V.P., Kessarkar, P.M., Krumbein, W.E., Krajewski, K.P., and Schneider, R.J., 2003, Microbial dolomite crusts from the carbonate platform off western India: Sedimentology, v. 50, p. 819–830.

Reddering, J.S.V., 1987, Subtidal occurrence of ladderback ripples: their significance in paleoenvironmental reconstructions: Sedimentology, v. 34, p. 253–257.

Reid, R.P., Macintyre, I.G., Browne, K.M., Steneck, R.S., and Miller, T., 1995, Stromatolites in the Exuma Cays, Bahamas: uncommonly common: Facies, v. 33, p. 1–18.

Reid, R.P., Visscher, P.T., Decho, A., Stolz, J.K., Bebout, B.M., Dupraz, C., Macintyre, I.G., Paerl, H.W., Pinchney, J.L., Prufert-Bebout, L., Steppe, T.F., and Des Marais, D.J., 2000, The role of microbes in accretion, lamination and early lithification of modern marine stromatolites: Nature, v. 406, p. 989–992.

Riding, R., 1994, Evolution of algal and cyanobacterial calcification, *in* Bengtson, S., ed., Early Life on Earth: Nobel Symposium, Columbia University Press, v. 84, p. 426–438.

Riding, R., 2000, Microbial carbonates: the geological record of calcified bacterial–algal mats and biofilms: Sedimentology, v. 47, p. 179–214.

Riding, R., 2011, Microbialites, stromatolites, and thrombolites, *in* Reitner, J., and Thiel, V., eds., Encyclopedia of Geobiology: Berlin, Springer, Encyclopedia of Earth Science Series, p. 635–654.

Riding, R., and Awramik, S.M., 2000, Microbial Sediments, Berlin, Springer, 327 p.

Riding, R., and Tomas, S., 2006, Stromatolite reef crusts, Early Cretaceous, Spain: bacterial origin of *in-situ* precipitated peloid microspar?: Sedimentology, v. 53, p. 23–34.

Riding, R., Awramik, S.M., Winsborough, B.M., Griffin, K.M., and Dill, R.F., 1991, Bahamian giant stromatolites: microbial composition of surface mats: Geological Magazine, v. 128, p. 227–234.

Sánchez-Román, M., Vasconcelos, C., Schmid, T., Dittrich, M., McKenzie, J.A., Zenobi, R., and Rivadeneyra, M.A., 2008, Aerobic microbial dolomite at the nanometer scale: implications for the geologic record: Geology, v. 36, p. 879–882.

Sarg, J.F., 2001, The sequence stratigraphy, sedimentology, and economic importance of evaporite–carbonate transitions: a review: Sedimentary Geology, v. 140, p. 9–42.

Schidlowski, M., 2000, Carbon isotopes and microbial sediments, *in* Riding, R.E., and Awramik, S.M., eds., Microbial Sediments: Berlin, Springer, p. 84–95.

Seong-Joo, L., Browne, K.M., and Golubic, S., 2000, On stromatolite lamination, *in* Riding, R.E., and Awramik, S.M., eds., Microbial Sediments: Berlin, Springer, p. 16–24.

Słowakiewicz, M., and Mikołajewski, Z., 2011, Upper Permian Main Dolomite microbial carbonates as potential source rocks for hydrocarbons (W Poland): Marine and Petroleum Geology, v. 28, p. 1572–1591.

Smith, D.B., 1981, The Magnesian Limestone (Upper Permian) Reef Complex of North eastern England: Society of Economic Paleontologists and Mineralogists, Special Publication, v. 30, p. 187–202.

Smith, D.B., 1986, The Trow Point Bed: a deposit of Upper Permian marine oncoids, peloids and stromatolites in the Zechstein of NE England, *in* Harwood, G.M., and Smith, D.B., eds., The English Zechstein and Related Topics: Geological Society of London, Special Publication 22, p.113–125.

Smith, D.B., 1995, Marine of Permian England: Geological Conservation Review Series, Chapman & Hall, 205 p.

Spadafora, A., Perri, E., McKenzie, J.A., and Vasconcelos, C., 2010, Microbial biomineralization processes forming modern Ca:Mg carbonate stromatolites: Sedimentology, v. 57, p. 27–40.

Tucker, M.E., 1991, Sequence stratigraphy of carbonate–evaporite basins: models and application to the Upper Permian (Zechstein) of northeast England and adjoining North Sea: Geological Society of London, Journal, v. 148, p. 1019–1036.

Tucker, M.E., and Hollingworth, N.T.J., 1986, The Upper Permian reef complex (EZ1) of North East England: diagenesis in a marine to evaporitic setting, *in* Schroeder, J.H., and Purser, B.H., eds., Reef Diagenesis: Berlin, Springer-Verlag, p. 270–290.

Van Lith, Y., Warthmann, R., Vasconcelos, C., and McKenzie, J.A., 2003a, Microbial fossilization in carbonate sediments: a result of the bacterial surface involvement in dolomite precipitation: Sedimentology, v. 50, p. 237–245.

Van Lith, Y., Warthmann, R., Vasconcelos, C., and McKenzie, J.A., 2003b, Sulphate-reducing bacteria induce low-temperature Ca-dolomite and high Mg-calcite formation: Geobiology, v. 1, p. 71–79.

Vasconcelos, C., McKenzie, J.A., Bernasconi, S., Grujic, D., and Tien, A.J., 1995, Microbial mediation as a possible mechanism for dolomite formation: Nature, v. 377, p. 220–222.

Veizer, J., Bruckschen, P., Pawellek, F., Diener, A., Podlaha, O.G., Carden, G.A.F., Jasper, T., Korte, C., Strauss, H., Azmy, K., and Ala, D., 1997, Oxygen isotope evolution of Phanerozoic sea water: Palaeogeography, Palaeoclimatology, Palaeoecology, v. 132, p. 159–172.

Veizer, J., Ala, D., Azmy, K., Bruckschen, P., Buhl, D., Bruhn, F., Carden, G.A.F., Diener, A., Ebneth S, Godderis, Y., Jasper, T., Korte, C., Pawellek, F., Podlaha, O., and Strauss, H., 1999, $^{87}Sr/^{86}Sr$, $\delta^{13}C$ and $\delta^{18}O$ evolution of Phanerozoic seawater: Chemical Geolology, v. 161, p. 59–88.

Visscher, P.T., and Stolz, J.F., 2005, Microbial mats as bioreactors: populations, process, and products: Palaeogeography, Palaeoclimatology, Palaeoecology, v. 219, p. 87–100.

Visscher, P.T., Reid, R.P., Bebout, B.M., Hoeft, S.E., Macintyre, I.G., and Thompson, J.A., 1998, Formation of lithified micritic laminae in modern marine stromatolites (Bahamas): the role of sulfur cycling: American Mineralogist, v. 83, p. 1482–1493.

Warren, J.K, 2006, Evaporites: Sediments, Resources, Hydrocarbons: Berlin, Springer-Verlag, 1035 p.

Wasson, M.S., Saller, A., Andres, M., Self, D., and Lomando, A., 2012, Lacustrine microbial carbonate facies in core from the Lower Cretaceous Toca Formation, Block 0, Offshore Angola: American Association of Petroleum Geologists, Hedberg Conference, Microbial Carbonate Reservoir Characterization, Houston, Texas, p. 140–143.

Wright, D.T., 1999, The role of sulphate-reducing bacteria and cyanobacteria in dolomite formation in distal ephemeral lakes of the Coorong region, South Australia: Sedimentary Geology, v. 126, p. 147–157.

Wright, D.T., and Wacey, D., 2005, Precipitation of dolomite using sulphate-reducing bacteria from the Coorong Region, South Australia: significance and implications: Sedimentology, v. 52, p. 987–1008.

Ziegenbalg, S.B. Brunner B., Rouchy, J.M., Birgel, D., Pierre, C., Böttcher, M.E., Caruso, A., Immenhauser, A., and Peckmann, J., 2010, Formation of secondary carbonates and native sulphur in sulphate-rich Messinian strata Sicily: Sedimentary Geology, v. 227, p. 37–50.

Received 7 March 2012; accepted 23 April 2013.